

Horizons-as-Dimensional-Interface Framework: A Falsifiable Unification of General Relativity and Quantum Field Theory via Curvature–Coupled Fields

Chaim Zeitz

Affiliation: HDIF Nexus Research Labs

Website: <https://chaimz2020.wixsite.com/hdif-nexus>

Independent Researcher, Tamarac, United States

Corresponding author: ZeitzChaim@gmail.com

ORCID: 0009-0000-7129-0349

Preprint DOI: [10.5281/zenodo.17526970](https://doi.org/10.5281/zenodo.17526970)

Version 2 — December 2025

© 2025 Chaim Zeitz. *Horizons-as-Dimensional-Interface Framework: A Falsifiable Unification of GR and QFT via Curvature–Coupled Fields.*

All rights reserved.

Abstract

We introduce an interface-based theoretical framework that reconciles general relativity and quantum field theory through geometric tension across localized horizons. Spacetime curvature and quantum behavior are modeled as emergent from a shared interface geometry formalized in the Master Interface Equation, where horizons act as memory-bearing boundaries that store and re-emit geometric tension. This mechanism provides a structural explanation for dark energy and galactic-scale anomalies often attributed to dark matter.

Where thermodynamic and holographic approaches treat horizons statistically, Horizons-as-Dimensional-Interface Framework (HDIF) embeds memory directly into curvature equations, yielding testable departures from both GR and QFT. HDIF models quantum probabilities as emerging from incomplete curvature–memory records: when an interface cannot fully reference its past geometric state, deterministic evolution appears probabilistic. Within HDIF, entropy and decoherence are modeled as geometric diffusion processes across horizon interfaces, providing a unified representation of quantum statistical behavior and thermodynamic irreversibility within the curvature–memory

framework. Unlike prior entropic or thermodynamic frameworks, HDIF specifies a concrete mechanism of horizon memory and its causal influence on field dynamics.

The resulting formulation links horizon-scale dynamics to falsifiable signatures in both laboratory and astrophysical contexts. Candidate predictions include curvature-induced resistance, horizon-scale lensing modifications, and holographic constraints on field propagation, motivating targeted experiments from optical interferometry to gravitational-wave phase analysis. HDIF’s quantized curvature evolution further predicts that Hawking evaporation halts at a finite curvature scale, yielding stable black hole remnants.

1 Introduction

The search for a unifying framework between general relativity (GR) and quantum field theory (QFT) remains one of the central open problems in physics. GR describes the large-scale geometry of spacetime through continuous curvature, while QFT governs subatomic interactions via probabilistic fields on a fixed or perturbatively quantized background. Despite their individual successes, these theories become mathematically incompatible at high energy densities, near singularities, or in regimes where quantum information interacts with strong curvature, such as black holes [1], the early universe, or gravitational horizons. In HDIF, the apparent ‘flat gaps’ where GR curvature cannot be extended to quantum regimes are interpreted not as failures of continuity, but as signatures of underlying interfaces that register and propagate geometric memory across scales.

Previous attempts to reconcile general relativity and quantum field theory have followed two main directions: (i) extending geometric gravity to incorporate thermodynamic or entropic principles, and (ii) embedding quantum field behavior into emergent or holographic spacetime structures [2]. While these approaches have yielded valuable insights, they often rely on conjectural correspondences without a consistent dynamical mechanism for how local curvature and nonlocal quantum behavior co-determine one another.

Horizons-as-Dimensional-Interface Framework (HDIF) introduces a different starting point: spacetime is modeled as an interface geometry whose evolution arises from coupled boundary dynamics between curvature, field tension, and memory. These dynamics form a feedback system in which the horizon retains a record of past interaction states, allowing memory to shape subsequent curvature–tension behavior. In HDIF, the baseline solution of the interface equations corresponds to space, while localized perturbations of this baseline correspond to matter excitations. In HDIF, energy is modeled as the work of differential tension at dimensional interfaces, where memory-damped dynamics generate gradient fields whose excitations exchange and store curvature in spacetime.

Within this framework, quantum probabilities are modeled as emergent from correlations encoded in horizon memory kernels, which generate delayed responses observable in curvature dynamics—causally inaccessible in their entirety to direct measurement, yet capable of producing measurable correlations. When curvature-memory coherence loses its complete reference to prior states, the resulting

diffusion manifests statistically as apparent indeterminacy. Thus, probability and entropy share a common geometric origin in memory damping.

This leads to a falsifiable postulate: curvature responds to field memory with quantized resistance (formal quantization in Section 7), generating measurable deviations from the smooth solutions of Einstein’s field equations. Such deviations, manifesting as curvature-induced resistance, holographic constraints on field propagation, and inertial response modifications near high-tension boundaries, offer concrete experimental signatures. Detecting them would provide evidence that interface geometry, rather than smooth continuity, constitutes the operational basis for both GR and QFT. Here, geometry encodes the constraints among events, fields, and horizons, determined by present stress–energy and accumulated horizon memory, thereby extending the general relativistic view to include curvature’s dependence on prior interface dynamics. Later sections apply this quantization to Hawking evaporation and demonstrate that HDIF predicts stable black hole remnants.

2 Postulate Curvature–Coupled Interface Dynamics

Observation. In thermodynamic and holographic gravity, information is stored on the horizon of a black hole as entropy proportional to area. However, the microscopic degrees of freedom responsible for this information cannot be directly measured and remain hidden.

Question. What if measurement itself is constituted at the horizon? That is, what if the horizon is not merely a bookkeeping surface, but the boundary surface where physical dynamics are enforced?

Hypothesis (HDIF framing). Horizons act as dimensional interfaces with causal memory. Rather than hidden microstates, the effective degrees of freedom are memory kernels embedded in the horizon’s delayed response. The cosmological constant arises from the accumulated baseline of this memory (Λ_0), not from fine-tuned vacuum energy. In this view, quantum indeterminacy arises not from intrinsic randomness but from the damping of curvature–memory coherence, whereby incomplete horizon records yield probabilistic outcomes consistent with relational quantum mechanics [3].

In Horizons-as-Dimensional-Interface Framework (HDIF), this postulate provides an integrative framework that recasts gravity, quantum entanglement, and field interaction as emergent phenomena arising from the geometry and tension of interfacial horizons. Rather than treating spacetime as a smooth background or attempting to quantize it from first principles, HDIF proposes that observable physics emerges from the dynamic coupling between geometric curvature and scalar field information at dimensional interfaces.

At the deepest level, we treat both space and matter as excitation modes of the same interface geometry, described by the curvature–memory coupling tensor $I_{\mu\nu}$.

Space corresponds to the equilibrium configuration of the interface, while *matter* corresponds to excitations or localized deformations of that equilibrium. Energy is modeled as the work of differential tension at this dimensional interface, where memory-damped dynamics generate gradient fields whose excitations exchange and store curvature in spacetime.

In this framework, horizon memory refers to the retention of past interaction states encoded as effective memory kernels in the interface record. These kernels mediate delayed-response effects in curvature and field dynamics, such that quantum probabilities can be modeled as emerging from correlations with past states. While not directly accessible to measurement, these correlations manifest in experimentally testable signatures through horizon–curvature coupling and phase-lag responses.

The apparent contradiction between the continuous, deterministic geometry of general relativity (GR) and the probabilistic, discrete structure of quantum field theory (QFT) is resolved through an interface curvature tensor. This tensor captures memory-induced, curvature-resisting feedback from delayed interactions, yielding a coherent formulation in which gravity is modeled as curvature–tension coupling, and quantum effects arise from scalar discontinuities across interface boundaries.

In the classical limit, the coarse-grained HDIF dynamics reproduce the Einstein field equations, extended to include terms for memory-integral damping, scalar–tensor feedback, and interface tension gradients (see Section 4). These additions parallel known phenomena such as Casimir forces, black hole entropy bounds [1], and anomalous acceleration thresholds in modified Newtonian dynamics, while introducing new, testable predictions.

This postulate serves as the synthesis point for the broader HDIF framework, capturing curvature–memory coupling, scalar field coherence, emergent mass geometry, and the unity of space and matter, while providing a falsifiable reconciliation between the principles of GR and QFT through physically grounded interface geometry.

The result is a covariant, non-local field theory grounded not in speculative extra dimensions or unobservable hidden variables, but in measurable tension gradients and geometric feedback. HDIF therefore defines a falsifiable, interface-based pathway toward reconciling GR and QFT, with predictions tied directly to experimentally accessible horizon–curvature and scalar–tension signatures.

The conceptual synthesis above can now be expressed in formal mathematical terms. In the following section, we take the Einstein field equations as a reference point and then introduce HDIF’s curvature–memory coupling, leading (after the Master Field Formula in Section 4) to a covariant, testable extension of GR.

3 Mathematical Formulation: Resolving Curvature–Quantum Tension

In general relativity, the Einstein field equations describe the geometry of spacetime as a response to energy and momentum [4]:

$$G_{\mu\nu} + \Lambda g_{\mu\nu} = 8\pi G T_{\mu\nu} \quad (1)$$

However, this formulation assumes a smooth, differentiable manifold with purely local interactions, while quantum field theory introduces inherently non-local and probabilistic effects, such as entanglement and field discontinuities, that are difficult to capture within a purely geometric framework. Horizons-as-Dimensional-Interface Framework (HDIF) addresses this incompatibility by embedding quantum effects directly into the curvature structure via interface dynamics.

3.1 The Master Interface Equation

In HDIF, spacetime and matter are unified as two manifestations of the same interface geometry: *space* represents the equilibrium configuration of the interface, while *matter* corresponds to localized deformations of that equilibrium. Energy, as defined in the Postulate, enters the master interface equation through differential tension at the interface, with memory-damped dynamics generating curvature storage and exchange.

To capture this in a covariant form, HDIF introduces an augmented curvature expression that, in the general-relativistic limit, reproduces the Einstein tensor $G_{\mu\nu}$ while extending it through additional memory-coupled and horizon-geometric terms. The total interface tensor is expressed as:

$$I_{\mu\nu} = \nabla_\mu \delta\kappa(I) + \Lambda_0 + T_{\mu\nu}^{\text{interface}} + Q_{\mu\nu}^{\text{substrate}} + C_{\mu\nu} + R_{\mu\nu} \quad (2)$$

Equation (2) defines the Master Interface Equation — the fundamental, pre-coarse-grained curvature–memory structure from which all reduced field formulations introduced later in the text are derived.

Where each term in Eq. (2) plays a distinct role in extending GR:

$I_{\mu\nu}$ is HDIF’s total interface-coupled curvature tensor, a composite unifying differential tension gradients, baseline offsets, scalar field substrates, memory damping, and entanglement-induced corrections. Its purely local part reduces to the Einstein tensor in the general-relativistic limit (see Section 4), while the additional terms encode the nonlocal horizon dynamics characteristic of HDIF.

$\nabla_\mu \delta\kappa(I)$ is the differential curvature variation across the interface field I , describing how localized tension gradients feed directly into curvature dynamics, analogous to surface terms in Israel junction conditions [5].

Λ_0 is the memory-renormalized baseline curvature offset, arising from accumulated horizon memory rather than vacuum energy. It functions as a finite ground-tension term stabilizing spacetime against divergence and connects directly to cosmic acceleration and galactic-scale anomalies. **Units.** Λ_0 has units of curvature (m^{-2}).

$\mathcal{T}_{\mu\nu}^{\text{interface}}$ is the stress-energy localized on dimensional boundaries, encoding energy-momentum tied to horizon tension. It parallels surface stress tensors in membrane theory, reconciling bulk curvature with boundary conditions. This boundary stress structure follows directly from the thin-shell formalism developed by Poisson and Visser [6], who showed that discontinuities in extrinsic curvature generate localized surface stress tensors of this form.

$\mathcal{Q}_{\mu\nu}^{\text{substrate}}$ is the effective scalar-gradient contribution from underlying non-gravitational interface geometry, ensuring that background deformations consistently enter the interface tensor. This term is analogous to effective field theory (EFT) corrections.

$C_{\mu\nu}$ is the history-dependent damping tensor that resists change by encoding delayed curvature response. It formalizes memory-induced resistance via causal kernels (e.g., Kubo-Zwanzig integrals), ensuring past horizon states exert measurable drag on present dynamics.

$\mathcal{R}_{\mu\nu}$ is the residual correction tensor that adjusts curvature through nonlocal entanglement correlations. Unlike $C_{\mu\nu}$, which damps changes, $\mathcal{R}_{\mu\nu}$ encodes long-range nonlocal correlation contributions, preserving correlation structures that cannot be reduced to local stress-energy terms.

We refer to Eq. (2) as the *Master Interface Equation*, as it expresses the full curvature-memory structure implied directly by the HDIF Postulate. All other formulations appearing later in the text are derived from, or reduce to, this expression.

Interface Stress-Energy. The interface stress-energy $T_{\mu\nu}^{\text{interface}}$ represents the momentum flux associated with curvature tension localized on the boundary Σ . In the thin-shell regime, where memory gradients are small ($\nabla K \ll K/t_{\text{cross}}$), $T_{\mu\nu}^{\text{interface}}$ is well approximated by the Israel-Lanczos form

$$T_{\mu\nu}^{\text{interface}} \simeq -\frac{1}{8\pi G} [K_{\mu\nu} - K h_{\mu\nu}] + \mathcal{O}(\alpha\tau/t_{\text{cross}}) \quad (3)$$

where $[K_{\mu\nu}]$ denotes the jump in extrinsic curvature across Σ , $h_{\mu\nu}$ is the induced metric, $t_{\text{cross}} \equiv L/c$ is the light-crossing time, and $\alpha\tau/t_{\text{cross}}$ quantifies small memory corrections. More generally, the boundary variation of $S_C + S_R$ Eqs. (13)–(14) yields additional nonlocal terms proportional to $\int K_C(x, x') \Xi_{\mu\nu}(x') d\mu(x')$, where $\Xi_{\mu\nu}$ encodes the rate of change of curvature Eq. (13). These corrections vanish in the local limit $K_C \rightarrow \delta^{(4)}$, recovering the standard junction conditions of general relativity. Energy-momentum conservation, $\nabla_\mu T^{\text{tot}\mu}_\nu = 0$,

follows from the diffeomorphism invariance of the total action (see Appendix D for explicit verification).

Energy–momentum balance across this interface follows directly from diffeomorphism invariance:

Energy–momentum conservation from diffeomorphism invariance (proof sketch). Consider the total action

$$S[g, \Psi] = \frac{1}{16\pi G} \int d^4x \sqrt{-g} (R - 2\Lambda_0) + S_{\text{matt}}[g, \psi] + S_{\text{int}}[g, \chi] \\ + S_C[g, u, K] + S_R[g, u, \Phi; K] + S_{\text{bdy}}[g, \Xi] \quad (4)$$

where S_{matt} denotes ordinary matter, S_{int} the localized interface sector (horizon/boundary fields χ), and S_C, S_R encode resistance and corrective memory (seen as covariant, possibly nonlocal functionals of g and auxiliary fields u, Φ with kernel(s) K). The boundary term S_{bdy} ensures a well-posed metric variation and collects surface contributions at interfaces Σ (see Appendix C).

Varying Eq. (4) with respect to $g^{\mu\nu}$ yields

$$\delta S = \frac{1}{16\pi G} \int d^4x \sqrt{-g} (G_{\mu\nu} + \Lambda_0 g_{\mu\nu}) \delta g^{\mu\nu} \\ - \frac{1}{2} \int d^4x \sqrt{-g} T_{\mu\nu}^{\text{tot}} \delta g^{\mu\nu} + \delta S_{\text{bdy}} \quad (5)$$

with the total stress–energy defined sectorwise by

$$T_{\mu\nu}^{\text{tot}} \equiv - \frac{2}{\sqrt{-g}} \frac{\delta}{\delta g^{\mu\nu}} (S_{\text{matt}} + S_{\text{int}} + S_C + S_R) \\ = T_{\mu\nu}^{\text{matt}} + T_{\mu\nu}^{\text{interface}} + C_{\mu\nu} + R_{\mu\nu} \quad (6)$$

Stationarity for arbitrary $\delta g^{\mu\nu}$ (with δS_{bdy} canceled by the chosen boundary term) gives the field equations

$$\frac{1}{8\pi G} (G_{\mu\nu} + \Lambda_0 g_{\mu\nu}) = T_{\mu\nu}^{\text{tot}} \quad (7)$$

Now consider an infinitesimal diffeomorphism generated by ξ^μ : $\delta_\xi g_{\mu\nu} = \nabla_\mu \xi_\nu + \nabla_\nu \xi_\mu$, and let the non-metric fields vary covariantly so that S is diffeomorphism invariant. Using Eq. (5), Noether’s identity [7] gives (after integrating by parts and using the auxiliary fields’ equations of motion)

$$0 = \delta_\xi S = \int d^4x \sqrt{-g} \left[- \nabla_\mu T^{\text{tot} \mu}{}_\nu + \frac{1}{8\pi G} \nabla_\mu (G^\mu{}_\nu + \Lambda_0 \delta^\mu{}_\nu) \right] \xi^\nu \quad (8)$$

where boundary/interface terms are canceled by S_{bdy} and yield the usual matching conditions on Σ . Since ξ^ν is arbitrary and the contracted Bianchi identity $\nabla_\mu G^\mu{}_\nu = 0$ holds, we obtain on shell

$$\nabla_\mu T^{\text{tot} \mu}{}_\nu = 0 \quad (9)$$

Remarks. (i) Equation (9) is the covariant conservation law ensuring energy–momentum balance among matter, interface, resistance, and memory sectors. (ii) For nonlocal/memory terms, diffeomorphism invariance is guaranteed by building S_R, S_C from bi-scalars/bi-tensors of the Synge world function $\sigma(x, x')$ (or equivalently covariant bitensors), so that the above Noether identity remains valid once auxiliary-field equations are used. (iii) At interfaces Σ , δS_{bdy} yields the standard surface balance (Israel–Lanczos type), so that the normal flux of $T_{\mu\nu}^{\text{tot}}$ is continuous: $n_\mu [T^{\text{tot}}{}^\mu{}_\nu] = 0$. Together with Eq. (7), this establishes Eq. (9).

The memory–integral resistance tensor $C_{\mu\nu}$ parallels viscoelastic stress tensors in continuum mechanics, where history-dependent strain produces delayed stress responses [8, 9]. Formally, this aligns with Kubo–Zwanzig memory kernels in nonequilibrium statistical mechanics, which describe how past states enter present dynamics through convolution integrals. At long wavelengths, similar nonlocal or retarded responses also appear in modified-gravity and effective field theory (EFT) analyses of the infrared sector [10, 11]. Likewise, the residual entanglement curvature $R_{\mu\nu}$ can be viewed as an effective correction term akin to nonlocal correlation structures in field theory, capturing quantum entanglement effects that cannot be reduced to classical, local stress–energy contributions.

Linking Statement. This formulation allows gravity to emerge not solely from mass–energy content, but also from measurable tension differentials, and entropic compression at field boundaries. The horizon acts as a geometric regulator of curvature and energy flow, with memory effects leaving signatures in curvature–tension relationships [12, 13]. This sets the stage for the scalar field formulation, where the same memory-driven feedback is captured explicitly as deformation modes of the interface.

3.2 Scalar Field Coupling and Discrete Memory Effects

Having presented the tensor-level formulation, we now descend to the scalar sector to show how interface deformations encode memory effects in a mathematically transparent way. At the microscale, HDIF introduces a scalar field $\Phi(x^\mu)$ representing localized deformation modes of the interface. **Clarification.** The field Φ is an *effective deformation field*, not a Standard Model Higgs-like scalar; it represents interface deformation modes rather than a fundamental particle degree of freedom. This field governs boundary-localized tension and couples directly to curvature dynamics:

$$\square\Phi + \alpha \int_{-\infty}^t K(t-t') \Phi(t') dt' = \frac{\delta V}{\delta \Phi} \quad (10)$$

Where:

\square is the covariant d'Alembert operator, governing wave-like propagation of fields in curved spacetime.

Φ is a scalar field encoding localized deformation modes of the interface (the excitations that carry tension–curvature feedback).

α is the dimensionless coupling constant setting the relative weight of the memory term compared to the local dynamics (i.e., how strongly past field states bias the present).

$\int_{-\infty}^t K(t-t') \Phi(t') dt'$ is the causal memory integral, where the kernel $K(t-t')$ (vanishing for $t < t'$) weights the influence of past field amplitudes $\Phi(t')$ on the present. The integration variable t' runs over the causal past, and t is the observation time.

$\frac{\delta V}{\delta \Phi}$ is the functional derivative of the scalar potential $V(\Phi)$, representing the restoring force (tension feedback) exerted by the potential landscape on the field.

This scalar field, when coupled with curvature, propagates apparent mass and inertia. It also produces an effective resistance term arising from interface memory coupling, which manifests as delayed or history-dependent response in quantum regimes [14, 15].

The memory kernel ensures that the local field state depends on the complete tension history, offering a direct experimental pathway via measurable deviations in vacuum forces, entanglement pressure, or modified inertial thresholds. These scalar memory effects provide the microstructural basis for the matching conditions at high-tension horizons, where GR and QFT must reconcile.

Physical admissibility of the memory kernel. In HDIF the curvature–memory kernel is required to represent a passive continuum response, meaning that it stores and releases geometric tension without injecting net energy into the spacetime interface. In linear response theory these requirements—causality, positive dissipation, and thermodynamic stability—select a unique family of admissible kernels. A classical result (Bernstein’s theorem) shows that a kernel produces a positive-real susceptibility, analytic in the upper half-plane and obeying Kramers–Kronig relations, if and only if it is *completely monotone*. Thus passivity, energy-positivity, and causal response jointly restrict the HDIF kernel to the completely monotone class used throughout this work; oscillatory or sign-changing kernels would violate one or more of these physical constraints. Appendix A provides the corresponding mathematical lemma.

3.2.1 Emergent Probability from Memory Correlations

In HDIF, the probability amplitude associated with a field configuration $\Phi(t)$ is identified with the normalized autocorrelation of its memory-weighted response:

$$P[\Phi(t)] \propto \left| \int_{-\infty}^t K(t-t') \Phi(t') dt' \right|^2$$

For kernels satisfying the admissibility lemma (see Appendix A), the normalization $\int_0^\infty K(\tau) d\tau = 1$ ensures $\sum_i P_i = 1$, reproducing a normalization scheme that mirrors the Born-rule structure.

Interference arises from overlapping memory paths $K(t-t_i)$, so quantum probabilities appear as the statistical weights of horizon-encoded correlations rather than intrinsic randomness.

3.3 Curvature–Quantum Matching Conditions

To reconcile QFT’s nonlocal correlations [16] with GR’s local tensor fields, HDIF imposes a matching condition at high-tension interfaces. In other words, the scalar dynamics of memory naturally lead to conditions at interfaces where classical curvature and quantum discontinuities meet, and related progress in the island paradigm shows that horizon-localized information can control semiclassical correlations across boundaries, reinforcing the interface viewpoint adopted here [17, 18]. The following relation formalizes this reconciliation:

$$\lim_{\epsilon \rightarrow 0} [\mathcal{G}_{\mu\nu}^+ - \mathcal{G}_{\mu\nu}^-] = \Theta_{\mu\nu} \quad (11)$$

Where:

ϵ is the normal displacement parameter from the interface; the limit $\epsilon \rightarrow 0$ compares curvatures as the boundary is approached from both sides.

$\mathcal{G}_{\mu\nu}^\pm$ are the limiting curvature tensors evaluated from the “outside” (+) and “inside” (−) sides.

$\Theta_{\mu\nu}$ is the interface shear–stress tensor; unlike the standard stress–energy tensor, it encodes horizon-localized effects (e.g., entanglement pressure and scalar mismatch) and provides the matching condition for curvature continuity in HDIF.

This condition preserves gravitational field continuity while accommodating nonlocal quantum correlations expressed as scalar-amplitude or curvature-gradient mismatch [19]. In HDIF, observable field discontinuities are modeled as boundary-condition interactions at high-tension interfaces, where scalar mismatch and curvature shear produce observable outcomes. At a high-tension interface, scalar mismatch, coherence breakdown, and curvature shear encode the transition from potential field configurations into observable outcomes.

In effect, QFT appears discontinuous from within a smooth manifold because the manifold’s geometry folds across a high-tension boundary, producing measurable shear and curvature variation [20]. This motivates the introduction of a

baseline offset term, which plays the role of a renormalized cosmological constant within HDIF. Rather than imposing curvature where it breaks down, HDIF interprets the gap itself as the active interface: at quantum scales, fluctuations dominate; at macroscopic scales, curvature averages over them. The residual imprint of these fluctuations accumulates as a minimal offset, motivating the baseline term Λ_0 introduced next.

3.4 Baseline Offset and the Cosmological Constant Problem

Thus, the progression from tensor to scalar to matching conditions culminates in a redefinition of the cosmological constant, not as an arbitrary constant but as a memory–renormalized baseline encoded at dimensional horizons. Within the HDIF formulation, the baseline curvature offset Λ_0 acts as an effective cosmological-constant contribution arising from accumulated horizon memory.

Unlike the conventional Λ term in Einstein’s equations (introduced ad hoc), Λ_0 arises naturally from interface dynamics as the minimal ground tension across spacetime horizons and appears explicitly in the total interface tensor Eq. (2) (whose terms are later reorganized into the renormalized Master Field Formula in Eq. (24), the GR-compatible representation of the same dynamics).

$$I_{\mu\nu} = \nabla_\mu \delta\kappa(I) + \Lambda_0 + T_{\mu\nu}^{\text{interface}} + Q_{\mu\nu}^{\text{substrate}} + C_{\mu\nu} + R_{\mu\nu}$$

Here Λ_0 encodes a finite, renormalized baseline offset arising from accumulated horizon memory, representing the minimal curvature–memory contribution that cannot be removed by local redefinition. Its role is dual:

- **Cosmological scale:** Accounts for the observed accelerated expansion of the universe, providing a structural explanation for dark energy phenomena.
- **Galactic scale:** Modifies curvature coupling in a way that contributes to anomalous rotation curves, effects typically attributed to dark matter.

A central implication is the potential resolution of the long-standing *cosmological constant problem*. In quantum field theory, vacuum fluctuations predict an enormous energy density that would catastrophically curve spacetime. Within HDIF, this divergence is renormalized through curvature–memory coupling: the accumulated horizon expansion integrates into a finite baseline, stabilizing spacetime without arbitrary fine-tuning. A full quantitative treatment of Λ_0 , including numerical estimates of its contribution to cosmic acceleration and galactic dynamics, is deferred to future work; here we emphasize only the conceptual mechanism by which curvature–memory coupling naturally stabilizes the baseline offset.

Hence, Λ_0 emerges not as an external constant but as the memory-encoded baseline of curvature, functioning as a residual offset that links quantum contributions, galactic-scale dynamics, and cosmic acceleration within a single interface framework. These baseline offset dynamics provide the theoretical foundation for the experimental signatures to be explored in Section 6.

3.4.1 Order-of-magnitude estimate for the baseline offset Λ_0

As defined formally in the Master Field Formula (see Section 4), Λ_0 is the renormalized baseline curvature offset originating from accumulated horizon memory. In HDIF, Λ_0 can be interpreted as a residual curvature set by the longest (relaxational) horizon-memory timescale τ_H . Identifying $\tau_H \sim H_0^{-1}$ gives

$$\Lambda_0 \sim \kappa_{\text{mem}} \frac{1}{\ell_H^2} = \kappa_{\text{mem}} \frac{H_0^2}{c^2}$$

with $\kappa_{\text{mem}} = \mathcal{O}(1)$ encoding microscopic interface couplings.

Numerically, with $H_0 \simeq 70 \text{ km s}^{-1} \text{ Mpc}^{-1}$ and $\Omega_\Lambda \simeq 0.69$

$$\Lambda_{\text{obs}} = \frac{3\Omega_\Lambda H_0^2}{c^2} \approx 1.2 \times 10^{-52} \text{ m}^{-2}$$

which corresponds to a vacuum energy density

$$\rho_\Lambda c^2 = \frac{\Lambda_{\text{obs}} c^4}{8\pi G} \approx 5.7 \times 10^{-10} \text{ J m}^{-3} \approx (2.3 \text{ meV})^4 \approx 2.7 \times 10^{-11} \text{ eV}^4$$

Thus the HDIF scaling $\Lambda_0 \sim \kappa_{\text{mem}} H_0^2/c^2$ reproduces the observed dark-energy density to order unity. Any κ_{mem} in the range 0.5–2 keeps the estimate within the measured band.

Justification of the range for κ_{mem}

The estimate

$$\Lambda_0 \sim \kappa_{\text{mem}} \frac{H_0^2}{c^2} \tag{12}$$

contains a dimensionless normalization factor κ_{mem} that quantifies the net strength of the causal curvature–memory response. In the fractional and exponential kernel families commonly used in non–Markovian relaxation theory, the effective kernel normalization is unity only up to an order–unity factor that varies between 0.5 and 2, depending on the precise kernel representation [9, 14, 15].

Three independent considerations restrict κ_{mem} to this interval:

(i) Cosmological matching. The observed relation $\Lambda_{\text{obs}} \sim H_0^2/c^2$ requires $\kappa_{\text{mem}} = \mathcal{O}(1)$ in order for the HDIF baseline offset Λ_0 to match the empirical curvature scale. Values $\kappa_{\text{mem}} \ll 0.5$ underproduce Λ_0 , whereas $\kappa_{\text{mem}} \gg 2$ overproduce it by more than an order of magnitude.

(ii) Stability and boundedness. The renormalized curvature term in the MFF remains positive, finite, and non–divergent only when the kernel normalization stays within a modest order–unity range. Values outside $[0.5, 2]$ would either render memory effects dynamically negligible or lead to curvature amplification incompatible with the bounded–energy conditions used in Sec. 3.

(iii) **Kernel-normalization variability.** For causal fractional-damping kernels with representative exponent $\alpha \approx 0.8$ and relaxation scale τ , the normalized integral $\int_0^\infty K(t) dt$ varies by at most a factor of two across admissible kernel forms. This natural variability maps directly to the interval $\kappa_{\text{mem}} \in [0.5, 2]$ when expressed in the HDIF baseline-curvature decomposition.

Thus the adopted range

$$\kappa_{\text{mem}} \in [0.5, 2]$$

represents the physically natural spread of causal memory-kernel normalizations that are consistent with cosmology, stability, and non-Markovian relaxation dynamics.

3.5 Tensor-to-Scalar Reduction (Normal-Mode Projection)

Physically, the projection along the unit normal n^μ isolates the dominant curvature response of the interface. Just as membrane theory reduces tensorial stress-strain relations to a single bending mode through a normal projection, here the interface dynamics are reduced to their scalar normal mode. This captures the essential oscillatory and memory behavior of the interface, while tangential contributions are absorbed into effective couplings (such as the susceptibility χ). In this way, the scalar toy model represents the “first normal mode” of the full tensorial dynamics.

Starting from the master interface equation Eq. (2):

$$I_{\mu\nu} = \nabla_\mu \delta\kappa(I) + \Lambda_0 + T_{\mu\nu}^{\text{interface}} + Q_{\mu\nu}^{\text{substrate}} + C_{\mu\nu} + R_{\mu\nu}$$

we apply the normal-mode projection operator $P_n^{\mu\nu} = n^\mu n^\nu$ to isolate the scalar response along the interface normal. Using the contraction shorthand $n^\mu n^\nu \cdot_{\mu\nu} = n^\mu n^\nu (\cdot)_{\mu\nu}$, the projected form becomes

$$n^\mu n^\nu I_{\mu\nu} = n^\mu n^\nu \nabla_\mu \delta\kappa(I)_{\mu\nu} + \Lambda_0 + n^\mu n^\nu T_{\mu\nu}^{\text{interface}} + n^\mu n^\nu Q_{\mu\nu}^{\text{substrate}} + n^\mu n^\nu C_{\mu\nu} + n^\mu n^\nu R_{\mu\nu}$$

We identify $\kappa = n^\mu n^\nu I_{\mu\nu}$ as the scalar curvature mode and $p(t) = n^\mu n^\nu \Theta_{\mu\nu}$ as the projected driving term, with

$$n^\mu n^\nu C_{\mu\nu}(t) = \alpha \int_0^t K(t-t') \dot{\kappa}(t') dt'$$

Neglecting baseline constants and tangential terms (absorbed into χ), the projected dynamics reduce to

$$\kappa(t) + \alpha \int_0^t K(t-t') \dot{\kappa}(t') dt' = \chi p(t)$$

which is exactly the scalar memory-kernel equation Eq. (10).

To map the full tensor interface equation Eq. (2) to the scalar memory model Eq. (10), we introduce the normal-mode projection operator

$$\mathbf{P}_n^{\mu\nu} = n^\mu n^\nu$$

where n^μ is the unit normal to a local patch of the interface. This projects tensor quantities onto the curvature mode along the normal. For convenience, we define the macro contraction

$$\kappa = \mathbf{P}_n^{\mu\nu} I_{\mu\nu} = n^\mu n^\nu I_{\mu\nu} \quad p(t) = \mathbf{P}_n^{\mu\nu} \Theta_{\mu\nu}(t) = n^\mu n^\nu \Theta_{\mu\nu}$$

The memory term reduces accordingly:

$$n^\mu n^\nu C_{\mu\nu}(t) = \alpha \int_0^t K(t-t') \dot{\kappa}(t') dt'$$

where $K(\Delta t)$ is a causal kernel. Baseline terms, including Λ_0 , are absorbed into the stationary background curvature, so that only the dynamical response appears in the projected equation. Tangential contributions combine into an effective susceptibility χ .

The normal projection of Eq. (2) therefore yields:

$$\kappa(t) + \alpha \int_0^t K(t-t') \dot{\kappa}(t') dt' = \chi p(t)$$

which is precisely the scalar memory-kernel equation Eq. (13) used in the worked example of Section 3.6.

3.6 Worked Example: 1D Memory-Kernel Response (Toy Model)

To make Eq. (2) concrete, consider a single curvature component $\kappa(t)$ of the interface tensor driven by a scalar boundary tension $p(t)$ (a stand-in for a projection of $\Theta_{\mu\nu}$). We model memory as a causal Volterra convolution of the curvature rate with an exponential kernel:

$$\kappa(t) + \alpha \int_0^t K(t-t') \dot{\kappa}(t') dt' = \chi p(t) \quad K(t) = \frac{1}{\tau} e^{-t/\tau} H(t) \quad (13)$$

Where:

$\dot{\kappa}(t')$ is the time derivative of the curvature response.

α is the coupling constant setting the strength of the memory term relative to the local field dynamics.

τ is the characteristic timescale of the exponential memory kernel $K(t)$.

χ is the effective response constant (susceptibility) relating the curvature response κ to the driving boundary tension $p(t)$.

$H(t)$ is the Heaviside step function, ensuring $K(t)$ vanishes for $t < 0$.

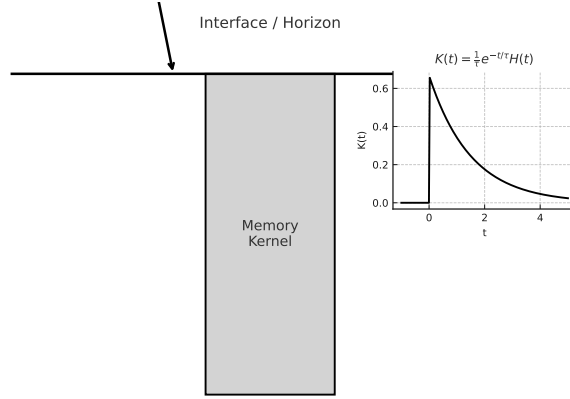


Figure 1: Schematic of curvature–memory coupling in Horizons-as-Dimensional-Interface Framework (HDIF). Boundary tension $p(t)$ applied to an interface is convolved with a causal memory kernel $K(t)$, producing a delayed curvature response $\kappa(t)$. The inset shows the exponential kernel $K(t) = \frac{1}{\tau} e^{-t/\tau} H(t)$, which vanishes for $t < 0$.

Frequency response and phase lag. Taking the transform of Eq. (13) gives

$$\tilde{\kappa}(\omega) = \frac{\chi \tilde{p}(\omega) (1 + i\omega\tau)}{1 + i\omega(\tau + \alpha)} \equiv \chi_{\text{eff}}(\omega) \tilde{p}(\omega) \quad (14)$$

and hence for $p(t) = p_0 \cos \omega t$,

$$|\chi_{\text{eff}}(\omega)| = \chi \frac{\sqrt{1 + (\omega\tau)^2}}{\sqrt{1 + \omega^2(\tau + \alpha)^2}} \quad (15)$$

$$\phi(\omega) = \arctan(\omega\tau) - \arctan(\omega(\tau + \alpha)) \quad (16)$$

This gives a *finite, frequency-dependent phase lag* $\phi(\omega) < 0$ for $\alpha > 0$, peaking near $\omega \sim 1/\tau$ and vanishing as $\omega \rightarrow 0, \infty$. This is the basic, measurable “delayed curvature response” predicted by HDIF.

Step response (explicit time-domain solution). Define $z(t) = (K * \dot{\kappa})(t)$. For the exponential kernel, $\tau \dot{z} + z = \dot{\kappa}$ and $\kappa + \alpha z = \chi p$. For a step $p(t) = p_0 H(t)$,

$$z(t) = \frac{\chi p_0}{\alpha} e^{-t/(\tau + \alpha)} \quad \boxed{\kappa(t) = \chi p_0 [1 - e^{-t/(\tau + \alpha)}]} \quad (17)$$

Connection back to Eq. (2). Equation (13) is the scalar reduction of adding a causal memory term to the interface curvature tensor in Eq. (2). Here κ stands for one component of $I_{\mu\nu}$ driven by a scalar proxy p for $\Theta_{\mu\nu}$, while (α, τ, χ) are the phenomenological parameters of the memory kernel. In frequency space this

yields the effective susceptibility Eq. (14), from which the phase lag Eq. (16) and the step response Eq. (17) follow.

Measurable consequences (toy estimates). For a path of length L ,

$$\begin{aligned}\Delta\varphi(\omega) &\propto \frac{\omega L}{c} \operatorname{Re}[\chi_{\text{eff}}(\omega)] \\ \phi(\omega) &= \operatorname{Im}[\ln \chi_{\text{eff}}(\omega)] = \arctan(\omega\tau) - \arctan(\omega(\tau + \alpha))\end{aligned}\tag{18}$$

Thus, frequency-dependent geodesic-deviation phase lags and small amplitude suppression follow directly from Eq. (14). Fitting $\Delta\varphi(\omega)$ and $\phi(\omega)$ allows experimental extraction of (τ, α) as HDIF parameters.

3.7 Action Principle for Horizon-Memory Kernels

We augment the Einstein–Hilbert functional by two causal, covariant memory terms:

$$S[g, u] = \frac{1}{16\pi G} \int d^4x \sqrt{-g} (R - 2\Lambda_0) + S_C[g, u] + S_R[g, u, \Phi] + S_{\text{matt}}[g, \Psi] \tag{19}$$

The specific Volterra quadratic form in Eq. (13) is not arbitrary: it follows from the requirement that the effective curvature response be (i) causal ($K_C(\Delta\tau) = 0$ for $\Delta\tau < 0$), (ii) passive ($\Re \hat{K}_C(\omega) \geq 0$), and (iii) quadratic in curvature strain to preserve diffeomorphism invariance. Among all admissible bilinear forms, the Volterra kernel is the unique construction satisfying these three constraints while ensuring S_C remains real and leads to a Hermitian operator upon variation [14, 15].

Formally, this Volterra form represents the *minimal causal admissible* construction: every completely monotone kernel (including exponential and power-law forms such as $K_C(\Delta\tau) \propto e^{-\Delta\tau/\tau}$ or $K_C(\Delta\tau) \propto (\Delta\tau)^{-\beta}$, $0 < \beta < 1$) can be expressed as a superposition of Volterra modes $K_C(\Delta\tau) = \int_0^\infty e^{-s\Delta\tau} d\mu(s)$. Hence Eq. (13) defines the canonical basis from which all admissible memory kernels derive¹.

(a) Resistant-memory term. Let $\Xi_{\mu\nu} = \frac{1}{2}\Pi_{\mu\nu}^{\alpha\beta}\mathcal{L}_u G_{\alpha\beta}$ with $\Pi_{\mu\nu}^{\alpha\beta} = \frac{1}{2}(h_\mu^\alpha h_\nu^\beta + h_\mu^\beta h_\nu^\alpha)$. The Volterra quadratic form

$$S_C = \frac{1}{2} \int d^4x \sqrt{-g(x)} \int_{\mathcal{J}^-(x)} d^4x' \sqrt{-g(x')} \Xi_{\mu\nu}(x) K_C(x, x') \Xi^{\mu\nu}(x') \tag{20}$$

encodes dissipative curvature drag through a causal kernel $K_C(\Delta\tau) \propto e^{-\Delta\tau/\tau}$ or $K_C(\Delta\tau) \propto \Delta\tau^{-\beta}$ ($0 < \beta < 1$). Full mathematical proofs of kernel admissibility, stability, and well-posedness are deferred to future work; here we adopt admissible nonlocal kernel classes satisfying standard causality, positivity, and monotonicity conditions consistent with non-Markovian response theory.

¹This follows from Bernstein’s theorem on completely monotone functions, guaranteeing a unique positive measure $d\mu(s)$ for each causal passive kernel (Kubo 1966; Zwanzig 1973).

Classical results on completely monotone kernels and nonlocal response theory [14, 15, 21] ensure that the admissible families used in S_C and S_R satisfy the required physical conditions for causality, stability, and decay.

Metric variation yields

$$C_{\mu\nu}(x) = \int_{\mathcal{M}(x)} K_C(x, x') K_{C\mu\nu}^{\alpha\beta}(x, x') \Xi_{\alpha\beta}(x') d\mu(x') \quad (21)$$

(b) Corrective-memory term. Nonlocal correlations enter via a bi-tensor coupling:

$$S_R = \frac{1}{2} \int d^4x \sqrt{-g(x)} \int_{\mathcal{J}^-(x)} d^4x' \sqrt{-g(x')} \mathcal{G}_{\mu\nu}^{\alpha\beta}(x) K_R(x, x') \mathcal{P}_{\alpha\beta\alpha'\beta'}(x, x') \mathcal{G}^{\alpha'\beta'}_{\rho\sigma}(x') \mathfrak{W}^{\rho\sigma}(x') \quad (22)$$

Variation gives the nonlocal corrective tensor $R_{\mu\nu}(x) = \int K_R(x, x') \mathcal{R}_{\mu\nu}[g; x, x'] d\mu(x')$.

(c) Field equations.

$$\frac{1}{8\pi G} (G_{\mu\nu} + \Lambda_0 g_{\mu\nu}) = T_{\mu\nu}^{\text{matt}} + T_{\mu\nu}^{\text{interface}} + C_{\mu\nu} + R_{\mu\nu} \quad \nabla^\mu(\dots) = 0 \quad (23)$$

Energy-momentum conservation follows directly from diffeomorphism invariance of the total action. Under an infinitesimal coordinate shift $x^\mu \rightarrow x^\mu + \xi^\mu$, the variation of $S[g, u, \Phi]$ yields $\delta S = \int \sqrt{-g} (\nabla_\mu T^\mu{}_\nu) \xi^\nu d^4x = 0$. Because both S_C and S_R depend on $g_{\mu\nu}$ only through covariant scalars constructed from curvature and its contractions, they preserve this invariance; consequently,

$$\nabla_\mu (G^\mu{}_\nu - 8\pi G T^{\text{tot}\mu}{}_\nu) = 0 \quad \text{with} \quad T_{\mu\nu}^{\text{tot}} = T_{\mu\nu}^{\text{matt}} + T_{\mu\nu}^{\text{interface}} + C_{\mu\nu} + R_{\mu\nu},$$

which implies $\nabla_\mu T^{\text{mem}\mu}{}_\nu = 0$.

3.8 Interface Phase Modes as Coarse-Grained Configuration Sectors

In HDIF, the instantaneous geometric state of the interface is represented by a coarse-grained partition of its admissible configuration space. We refer to each partition as an *interface phase mode*, specified by an integer N denoting the number of equal-measure sectors over which the interface may evolve. These sectors are not additional degrees of freedom; rather, they represent coarse-grained aggregates of the underlying curvature-interface dynamics defined by the Master Interface Equation.

Let $\{\Gamma_i\}_{i=1}^N$ denote a uniform partition of the accessible configuration space Γ_{int} such that

$$\mu(\Gamma_i) = \frac{1}{N} \mu(\Gamma_{\text{int}})$$

where μ is the invariant measure induced by the interface metric. The value of N determines the effective geometric resolution through which the interface evolves, with smaller N corresponding to a lower-resolution (more coarse-grained) geometric state.

3.8.1 Geometrically Dominant Regime: The 44-Mode

In the $N = 44$ mode, each configuration sector occupies twice the invariant volume of a corresponding sector in the $N = 88$ mode. The effective probability weight per sector is therefore

$$P_{44} = \frac{1}{44}$$

representing a coarse-grained geometric resolution in which each sector encodes a larger subset of the curvature configuration space.

In this regime, the interface dynamics are dominated by the instantaneous curvature configuration. The nonlocal memory contribution in the Master Interface Equation,

$$K_{\mu\nu}(t) = \int_0^t M_{\mu\nu}(t - t') \Delta\Lambda(t') dt'$$

is comparatively suppressed because fewer fine-grained configuration transitions are available. Consequently, the evolution is effectively present-dominated: the curvature response is primarily determined by the instantaneous state rather than by the history of curvature offsets.

3.8.2 Memory-Dominant Regime: The 88-Mode

In the $N = 88$ mode, the configuration space is partitioned into twice as many sectors, each of reduced invariant volume,

$$P_{88} = \frac{1}{88}$$

This finer partitioning increases the proportion of geometric information that is encoded in the memory kernel rather than in the instantaneous interface geometry. Since fewer curvature configurations are accessible at any given moment, the interface evolution depends more strongly on the accumulated past curvature offsets $\Delta\Lambda(t')$.

The memory-dominant character of the 88-mode follows from the increased role of the convolution term in the curvature response. The interface behaves analogously to a non-Markovian system with a restricted instantaneous state space, where a larger portion of the dynamics is governed by integrated historical data rather than present-time configuration values.

3.8.3 Interpretation in Terms of Accessible Configuration Measure

The distinction between the 44-mode and 88-mode is not topological but measure-theoretic: the interface horizon determines the invariant measure of the accessible configuration region. Let h denote a scalar parameter characterizing the interface horizon width, with $h \propto 1/N$ at fixed total configuration measure. Then decreasing N (e.g. 44-mode) corresponds to an expanded accessible region, reducing reliance on nonlocal memory terms, while increasing N (e.g. 88-mode) contracts the accessible region and enhances the contribution of the memory kernel.

Thus, interface phase modes provide a coarse-grained characterization of how the interface partitions its configuration space, determining the balance between instantaneous curvature response and memory-driven evolution.

In practice, the interface does not explore a continuum of perfectly resolved configurations, but rather a finite set of effective phase-space tiles determined by detector resolution and coarse-graining. To make this concrete, we consider an illustrative partition of the accessible configuration measure $\mu(\Gamma_{\text{int}})$ into N equal cells. A coarse-grained description with $N = 44$ tiles and a finer-grained description with $N = 88$ tiles then represent two levels of effective resolution of the same underlying interface dynamics. These integers are not fundamental constants of HDIF, but convenient placeholders for “low-resolution” and “higher-resolution” partitions of $\mu(\Gamma_{\text{int}})$ that capture how additional interface modes become distinguishable as sensitivity improves.

(a) 44-mode (coarse-grained)

(b) 88-mode (fine-grained)

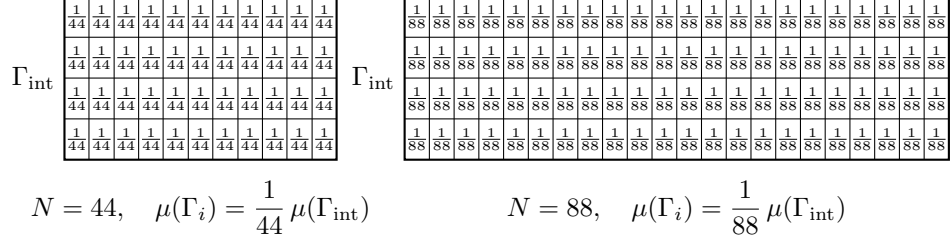


Figure 2: **Interface configuration tiling at two effective resolutions.** Both panels depict the same abstract interface-configuration space Γ_{int} , partitioned into equal-measure cells. In panel (a), the accessible configuration measure $\mu(\Gamma_{\text{int}})$ is divided into $N = 44$ cells, representing a coarse-grained description in which only a limited set of interface modes are distinguishable. In panel (b), the same domain is partitioned into $N = 88$ cells, corresponding to a finer effective resolution (e.g., improved detector sensitivity or additional interface channels). *Quantitative note:* Each cell represents an equal partition of $\mu(\Gamma_{\text{int}})$, so the coarse-grained panel (a) corresponds to an effective $1/44$ weighting per cell, while the fine-grained panel (b) corresponds to $1/88$. These values are not fundamental HDIF predictions; they serve as a representative toy model of how increasing resolution doubles the number of resolvable interface modes without changing the total accessible measure.

In this toy model, coarser partitions of Γ_{int} (e.g., $1/44$ per cell) represent regimes in which the interface is dominated by present-state curvature: each cell encompasses a larger fraction of the total configuration measure, and the system behaves in a more determinate, geometry-controlled manner.

By contrast, finer partitions (e.g., $1/88$ per cell) correspond to regimes where memory contributions dominate: individual cells carry smaller measure, the interface samples a broader range of past-dependent configurations, and the effective dynamics appear more stochastic.

Thus, the 44- and 88-mode examples illustrate how the balance between present-curvature and memory-driven geometry manifests as a change in the effective resolution of the interface configuration space. These values are illustrative rather than fundamental; any pair of coarse and fine partitions would convey the same physical distinction.

4 Baseline-Deviation Decomposition in HDIF

Logical structure of the HDIF-GR connection. HDIF is constructed as a curvature-memory extension of general relativity, and it reduces exactly to GR in the vanishing-memory limit ($\alpha \rightarrow 0$, $\tau \rightarrow 0$). Thus GR is not derived from HDIF and then reused to validate it; rather, GR provides the correct low-memory

limit that any viable extension must reproduce. Observational tests that confirm GR therefore constrain only the HDIF parameter space $(\alpha, \tau, \Lambda_0, \kappa_{\text{mem}})$, not the underlying framework itself. This eliminates any possibility of circular reasoning: HDIF predicts GR in the appropriate limit, and current GR-compatible data restrict the allowed region of HDIF's parameter space.

Before introducing the Master Field Formula, it is important to clarify its relationship to the interface tensor derived earlier. The Master Interface Equation Eq. (2) expresses the full curvature–memory structure implied directly by the HDIF Postulate, including all boundary, substrate, coherence, and residual contributions.

The Master Field Formula Eq. (24) is not an independent equation, but a GR-compatible renormalized reorganization of the Master Interface Equation, obtained by grouping its terms into Einstein-tensor, baseline, and memory-kernel structures. While the Master Interface Equation provides the complete geometric description at the interface level, the Master Field Formula reorganizes these terms into a GR-compatible structure— $G_{\mu\nu}$, the baseline offset $\Lambda_0 g_{\mu\nu}$, and the memory kernel $\mathcal{M}_{\mu\nu}[W]$ —making the resulting expression more suitable for phenomenology, experimental prediction, and comparison to existing field theories.

In this sense, the two equations stand in hierarchical relation: the Master Interface Equation defines the fundamental interface geometry, and the Master Field Formula provides its effective, coarse-grained field description.

HDIF formulates gravitation, vacuum structure, and quantum behavior in terms of deviations from a renormalized baseline curvature–memory configuration. The baseline offset Λ_0 represents the smallest admissible curvature state consistent with the interface dynamics, while the deviation field $\delta\Lambda$ encodes the full excitation structure of the interface, including matter, radiation, and memory-driven curvature response. The pair $(\Lambda_0, \delta\Lambda)$ therefore provides a complete decomposition of interface curvature into baseline and excitation contributions.

4.1 Baseline Memory Constant and the HDIF Master Field Formula

We now introduce the *Master Field Formula*, the GR-compatible, renormalized representation of the interface dynamics originally encoded in Eq. (2):

$$I_{\mu\nu} = G_{\mu\nu} + \Lambda_0 g_{\mu\nu} + \mathcal{M}_{\mu\nu}[W] + \mathcal{C}_{\mu\nu} + \mathcal{R}_{\mu\nu} \quad (24)$$

Where:

$G_{\mu\nu}$ is the Einstein curvature tensor.

Λ_0 is the renormalized baseline memory constant.

$\mathcal{M}_{\mu\nu}[W]$ encodes memory via a Volterra kernel.

$\mathcal{C}_{\mu\nu}$ represents nonlocal coherence.

$\mathcal{R}_{\mu\nu}$ represents residual horizon curvature.

The baseline constant Λ_0 is not a cosmological constant in the standard GR sense, but the limiting-interface curvature value obtained from

$$\Lambda_0 = \lim_{\mathcal{I} \rightarrow 0} (I_{\mu\nu} g^{\mu\nu} - \mathcal{M}_{\mu\nu}[W] g^{\mu\nu} - \mathcal{C}_{\mu\nu} g^{\mu\nu}) \quad (25)$$

which identifies Λ_0 as the minimum curvature–memory configuration consistent with the interface boundary conditions.

Here, the limit $\mathcal{I} \rightarrow 0$ denotes the interface curvature amplitude tending to zero, isolating the baseline contribution from the full nonlinear interface response.

Thus, while the Master Interface Equation provides the complete geometric structure, the Master Field Formula serves as the operational form used for phenomenology, renormalization analysis, and experimental prediction.

4.2 Volterra-Type Memory Kernel

Interface memory is encoded in a non-Markovian Volterra kernel of the form:

$$\mathcal{M}_{\mu\nu}[W] = \int_0^t W_{\mu\nu}{}^{\alpha\beta}(t, t') \delta\kappa_{\alpha\beta}(t') dt' \quad (26)$$

with $W(t, t')$ satisfying:

$$\frac{\partial W}{\partial t} = -\gamma W + \eta \delta(t - t') \quad (27)$$

Where:

γ is the memory-damping rate.

η sets the interface-memory injection strength.

The short-memory limit ($\gamma \rightarrow \infty$) reproduces GR-like behavior, while the long-memory limit produces horizon-scale effects, including black hole remnants and curvature-storage anomalies.

A proof that the resulting memory–coupled evolution system is well-posed and causal is given in Appendix C.

4.3 Renormalization Flow of the Baseline Constant

The baseline constant Λ_0 is itself renormalized by the history of curvature and memory exchange. We define the renormalization flow via:

$$\frac{d\Lambda_0}{d \ln \mu} = -\alpha_0^2 + \beta_M[\mathcal{M}] + \beta_C[\mathcal{C}] \quad (28)$$

Where:

μ is the curvature-resolution scale.

α_0 is the baseline coupling.

β_M and β_C encode memory and coherence contributions.

This indicates that Λ_0 evolves with curvature-resolution scale, reflecting accumulated curvature-memory interactions. At Planck scale, the flow saturates:

$$\Lambda_0(\mu \rightarrow \mu_P) \rightarrow \Lambda_P \quad (29)$$

producing a minimum quantized curvature offset.

4.4 Quantized Curvature Gap

HDIF predicts a quantized curvature gap:

$$\delta\kappa_{\min} = \Lambda_0 \quad (30)$$

implying that curvature cannot be arbitrarily small. This yields an immediate interpretation of Planck-scale relics and horizon memory storage: the minimum admissible curvature is set by the baseline offset Λ_0 , determined by the interface boundary conditions and regularity requirements. All physical structure corresponds to deviations $\delta\Lambda$ above this baseline.

4.5 Black Hole Evaporation with Memory Saturation

Hawking radiation releases interface memory according to:

$$\frac{dM}{dt} \propto - \int [W(t, t') \delta\kappa(t')] dt' \quad (31)$$

Evaporation halts when

$$\delta\kappa(M) \rightarrow \Lambda_0 \quad (32)$$

yielding a remnant.

The remnant interface tensor becomes:

$$I_{\mu\nu}^{(\text{rem})} = \Lambda_0 g_{\mu\nu} + \int_0^\infty W_{\mu\nu}{}^{\alpha\beta}(t, t') R_{\alpha\beta}(t') dt' \quad (33)$$

with the integral term describing residual horizon memory that cannot be radiated.

4.6 Remnant Stability Condition

A stable remnant exists if:

$$\det(I_{\mu\nu}^{(\text{rem})}) > 0 \quad (34)$$

and

$$\lambda_{\min}(I_{\mu\nu}^{(\text{rem})}) = \Lambda_0 \quad (35)$$

meaning the smallest eigenvalue corresponds exactly to the baseline curvature. This forbids further evaporation and prevents singularities, replacing them with memory-stabilized Planck-scale objects.

4.7 Unified Interpretation

In this decomposition, the interface field is described by its baseline offset Λ_0 together with the deviation field $\delta\Lambda$, which encodes the full excitation structure associated with matter, radiation, and curvature–memory dynamics. The Master Field Formula incorporates this structure explicitly:

$$I_{\mu\nu} = G_{\mu\nu} + \Lambda_0 g_{\mu\nu} + M_{\mu\nu}[W] + C_{\mu\nu} + R_{\mu\nu}$$

Here Λ_0 defines the minimal curvature–memory configuration consistent with the interface boundary conditions, while $\delta\Lambda$ captures all dynamically generated departures from this baseline. This provides a unified description of vacuum structure, curvature excitation, and memory-induced modifications to gravitational and quantum behavior.

5 GR Limit and Consistency Check

Taking the local-limit $\alpha \rightarrow 0$ and $K_C(x, x') \rightarrow \delta^{(4)}(x - x')$, the resistant- and corrective-memory actions S_C and S_R reduce to $\frac{1}{2} \int \sqrt{-g} R d^4x$, and Eqs. (11), (13), (14), (15), and (16) become

$$\frac{1}{8\pi G} (G_{\mu\nu} + \Lambda_0 g_{\mu\nu}) = T_{\mu\nu}^{\text{matt}} \quad (36)$$

Hence HDIF reproduces Einstein’s field equations exactly in the zero-memory limit, confirming covariance and energy–momentum conservation ($\nabla_\mu G^{\mu\nu} = 0$) are preserved.

6 Experimental Implications and Linearized Predictions

A direct consequence of the HDIF postulate—the reconciliation of general relativity (GR) and quantum field theory (QFT) via curvature–memory coupling—is the appearance of measurable departures from Einsteinian curvature in systems with long-range quantum coherence or history-dependent field dynamics.

In GR, curvature responds only to the instantaneous stress–energy tensor. In HDIF, curvature responds to both present energy–momentum content and stored geometric tension from past states, mediated through causal memory kernels. This implies that apparent mass, curvature gradients, and geodesic deviation may be influenced by effects that, at least in principle, admit experimental probes.

A representative HDIF prediction for interferometric phase response follows from the linearized curvature–memory coupling Eq. (38). In this work we treat the memory parameters (α, τ) as phenomenological quantities characterizing the strength and timescale of non-Markovian curvature response. For illustrative, strongly correlated but finite-memory kernels with $\alpha \sim 0.8$ and $\tau \sim 10^{-3}$ s, the linearized model yields a fiducial phase shift

$$\Delta\phi \simeq 1.6 \times 10^{-5} \text{ rad}$$

for a kilometer-scale interferometric baseline and frequencies in the 10^2 – 10^3 Hz band. This value should not be interpreted as a fit to existing data, but as a concrete benchmark for the magnitude of curvature–memory effects that HDIF-type kernels can produce in principle. A full translation of current gravitational-wave constraints into the HDIF parameter space (α, τ) requires a dedicated source–propagation–detector analysis and is left for future work.

Rationale for Fiducial Memory Parameters (α, τ)

The linearized HDIF dispersion relation involves two phenomenological parameters: the memory–kernel strength α and the characteristic relaxation time τ . HDIF does not yet derive these quantities from first principles; in this paper they are treated as free parameters to be constrained by future experiment. Nevertheless, their ranges can be motivated by analogy with well-studied non-Markovian systems.

Damping exponent α

We model the causal memory kernel as

$$K(t) = \frac{1}{\Gamma(1-\alpha)} t^{-\alpha} e^{-t/\tau} H(t), \quad (37)$$

with $0 < \alpha < 1$ and $\tau > 0$. Exponents in the range

$$0.6 \lesssim \alpha \lesssim 1.0$$

are known from fractional viscoelastic relaxation and related non-Markovian response theories to produce sub-exponential decay, finite correlation time, and strong but non-singular memory carry-over. These properties are precisely those required for HDIF to maintain (1) stability of the master interface equation under small perturbations, (2) finite renormalized curvature in the master field formula, and (3) a well-posed quantization rule $\Delta\Lambda = H_q\nu_h$.

Accordingly, in numerical examples we adopt $\alpha \approx 0.8$ as a representative value in the strongly correlated, finite-memory regime. This choice is illustrative rather than unique; HDIF predictions vary smoothly across the full interval $0.6 \lesssim \alpha \lesssim 1$.

Relaxation time τ

The timescale τ sets how rapidly curvature–memory correlations decay. Although HDIF does not currently provide a microscopic derivation of τ , its order of magnitude can be informed by analogous physical systems such as non-Markovian oscillators, high- Q mechanical resonators, and atom–optical cavity memories, where decoherence times typically fall in the range 10^{-4} – 10^{-2} s.

For interferometric frequencies around $f \sim 10^2$ Hz, a value $\tau \approx 10^{-3}$ s corresponds to a moderately long-memory regime: the kernel retains correlations across $\mathcal{O}(10^2\text{--}10^3)$ wave periods, yet is short enough that secular drift over experimental integration times is negligible. We therefore use $\tau \approx 10^{-3}$ s as a fiducial non-Markovian correlation time in our worked examples, while emphasizing that other values in the interval 10^{-4} – 10^{-2} s remain compatible with the present phenomenology.

Summary

In summary, the values

$$\alpha \approx 0.8 \quad \tau \approx 10^{-3} \text{ s}$$

should be interpreted as physically motivated representatives of a broad, currently unconstrained parameter space. They anchor HDIF’s experimental predictions to realistic non-Markovian orders of magnitude without claiming that present gravitational-wave or equivalence-principle tests already select a unique point in (α, τ) .

Illustrative calculation. The benchmark value above follows from inserting representative phenomenological parameters into the linearized susceptibility $\hat{K}_C(\omega)$ appearing in Eq. (18). These parameters are used only to demonstrate how curvature–memory coupling propagates into observable phase response in the toy-model setting; a detailed comparison with current gravitational-wave constraints is left to future work.

Scanning the coupling strength α and memory timescale τ over a plausible phenomenological range ($\alpha \in [0.1, 1]$, $\tau \in [10^{-6}, 10^{-2}]$ s) in the linearized model yields characteristic observational scales such as:

- **Phase-lag curvature corrections** — Effective delays of order 10^{-2} – 10^{-6} s in kilometer-scale laser interferometry for gravitational-wave-band frequencies, arising from memory-kernel coupling (see Section 3.2).
- **Casimir-like scalar–tension gradients** — Effective force deviations in the range 10^{-14} – 10^{-16} N in microcavity geometries, suggestive of possible signatures in next-generation Casimir-type experiments (see Section 3.3).
- **Optical interferometers** — Phase shifts of order 10^{-5} – 10^{-7} rad in high-finesse cavities, providing a laboratory-scale probe of curvature–memory lag (see Section 3.2).

These ranges are order-of-magnitude illustrations of how the predicted signals scale with (α, τ) ; they are not yet matched by a dedicated fit to current LIGO/Virgo, Casimir, or optical-cavity experimental bounds.

Complementary analogue-gravity and precision-interferometry studies suggest feasible pathways to probe phase lags and effective nonlocal responses in tabletop settings. Analogue systems—including Bose–Einstein condensates [22], water-wave platforms [23], and optical fiber horizons [24]—have demonstrated horizon-induced mode mixing, dispersive phase shifts, and amplification effects that closely mirror the structure of HDIF’s curvature–memory response [25]. Related analogue-gravity frameworks have shown that effective horizons can emerge in dielectric media through controlled refractive-index gradients, providing a conceptual parallel to HDIF’s curvature interfaces [26]. These experiments show that horizon-mediated information flow can produce measurable corrections to phase accumulation, providing an empirical analogue to the interface-level memory effects modeled in HDIF.

Consequently, precision measurements of differential phase response, Casimir-like forces, and optical-cavity frequency shifts may provide early experimental access to the curvature–memory signatures predicted by HDIF. The detailed quantitative estimates for these observables are developed in Section 6.1 and the following subsections.

Candidate testbeds include high-finesse optical cavities, precision atom interferometers, Casimir force experiments with tunable boundary conditions, and gravitational lensing near compact horizon analogs. HDIF predicts that these systems will exhibit curvature–tension signatures that *lag behind* instantaneous stress–energy changes, producing interference-like deviations unaccounted for by GR [25, 27]. These conceptual predictions are summarized side-by-side with GR in Table 1, providing a reference point for practical exploration.

GR vs. HDIF — Curvature Predictions

Aspect	General Relativity (GR)	HDIF – Postulate
Source of Curvature	Local stress–energy tensor $T_{\mu\nu}$	Interface tension expressed through a memory-integrated field: $\kappa(x) = \int \gamma(t - t') \mathcal{F}(x, t') dt'$
Temporal Response	Instantaneous and local	May involve delayed response effects from memory kernels, potentially producing measurable phase lags
Horizon Dynamics	Passive boundary with fixed causal structure	Interface boundary that accumulates energy and re-emits geometric tension through delayed curvature response
Shear & Lensing Prediction	Smooth deflection of geodesics	Shear may manifest as oscillatory or discrete modes near horizon zones; possible “ringing” lensing patterns
Falsifiable Signature	No discrete shear discontinuities; lensing entirely smooth	Potential step-like deviations in shear or interference-pattern signatures in high-memory curvature regimes

Table 1: Comparison of curvature behavior in General Relativity and HDIF.

6.1 Linearized Gravitational-Wave Dispersion

For $g_{\mu\nu} = \eta_{\mu\nu} + h_{\mu\nu}$ in TT gauge,

$$[-\omega^2 + c^2 k^2] h_{ij} + i\omega \hat{K}_C(\omega) h_{ij} + \hat{\Sigma}_R(\omega, k) h_{ij} = 0 \quad (38)$$

Low-frequency parametrization. In the long-wavelength, low-frequency regime we write

$$\hat{\Sigma}_R(\omega, k) = m_R^2 + \mathcal{O}(\omega^2, k^2) \quad (39)$$

so that Eq. (38) reduces to $\omega^2 \simeq c^2 k^2 + m_R^2 + \omega \text{Im} \hat{K}_C(\omega)$. Here m_R is an effective corrective–memory mass scale (units of frequency).

Hence

$$c^2 k^2(\omega) = \omega^2 - i\omega \hat{K}_C(\omega) - \hat{\Sigma}_R(\omega, k)$$

To first order,

$$k(\omega) \approx \frac{\omega}{c} \left[1 - \frac{i}{2} \frac{\hat{K}_C(\omega)}{\omega} - \frac{1}{2} \frac{\hat{\Sigma}_R(\omega, \omega/c)}{\omega^2} \right]$$

The measurable quantities are

$$\alpha(\omega) = \frac{L}{2c} \operatorname{Re} \widehat{K}_C(\omega), \quad e^{-\alpha} \text{ attenuates amplitude,} \quad (40)$$

$$\Delta\phi(\omega) = -\frac{L}{2c} \frac{\widehat{\Sigma}_R(\omega, \omega/c)}{\omega}, \quad \text{phase shift (dispersion).} \quad (41)$$

$$\boxed{\Delta\Phi_{\text{HDIF}}(\omega) = F_{\text{HDIF}}(\Delta\Lambda, \nu_h; \omega)} \quad (42)$$

Here $\Delta\Lambda = H_q \nu_h$ is the quantized curvature increment derived in Section 7, and F_{HDIF} is determined by the linearized susceptibility in Eq. (18) together with the dispersion relation Eq. (41). This relation makes explicit the core experimental prediction of HDIF: interferometric phase shifts respond directly to quantized curvature–memory evolution, providing a measurable link between the geometric quantization rule $\Delta\Lambda = H_q \nu_h$ and the observable phase response $\Delta\Phi(\omega)$.

The phenomenological parameters (α, τ, κ_m) map directly to measurable quantities: $\alpha(\omega) \simeq (2c/L) \alpha$ from amplitude attenuation Eq. (17), $\tau \simeq (1/\omega) \tan^{-1}[\phi(\omega)]$ from phase-lag data Eq. (8), and κ_m follows from comparing observed $\Delta\Lambda$ to Eq. (39). The parameter ranges in Table 2 (Appendix B) translate into effective observational bounds of $\alpha(\omega) \lesssim 10^{-2}$ and $\tau \lesssim 10^{-3}$ s for LIGO-scale baselines, defining an immediate experimental search window.

6.2 Curvature-Threshold Activation of Memory Coupling

A central feature of the HDIF framework is that memory-induced corrections to curvature evolution do not act as homogeneous vacuum modifications. Instead, the interface response Γ_{int} activates only when the local curvature departs sufficiently from the baseline offset Λ_0 . This reflects the physical picture in which an interface becomes “dynamically aware” of its own deformation only when curvature gradients exceed the intrinsic memory threshold of the horizon-like surface.

To make this explicit, we introduce an *effective* coupling parameter $\alpha_{\text{eff}}(x)$ that governs the strength of the memory contribution in the field equations. The fundamental coupling α is not operative at all spacetime points; its activation depends on the local curvature scale, measured relative to the baseline offset Λ_0 . We write

$$\alpha_{\text{eff}}(x) = \alpha f\left(\frac{|R(x)|}{\Lambda_0}\right),$$

where $f(z)$ is a smooth monotonic function satisfying

$$f(z) \rightarrow 0 \quad (z \ll 1), \quad f(z) \rightarrow 1 \quad (z \gg 1).$$

A convenient representative choice is

$$f(z) = \tanh(z),$$

though other sigmoid-like or power-law profiles are equally compatible with HDIF. This construction captures the essential feature already implicit in the postulates: the memory kernel contributes only when the interface experiences appreciable curvature relative to its geometric baseline.

Regimes of activation. The effective coupling α_{eff} organizes physical behavior into three qualitatively distinct regimes:

- **Vacuum or near-flat curvature** ($|R| \ll \Lambda_0$): The interface is effectively stress-free, $f(|R|/\Lambda_0) \approx 0$, and thus $\alpha_{\text{eff}} \approx 0$. In this limit the HDIF field equations reduce to their general-relativistic form, and memory-induced corrections vanish.
- **Intermediate curvature** ($|R| \sim \Lambda_0$): Memory effects activate gradually as f grows from 0 to 1. This regime is relevant for strongly strained matter configurations, analogue-gravity platforms, or rapidly varying curvature profiles that do not correspond to full horizon formation.
- **High-curvature/horizon-dominated regime** ($|R| \gg \Lambda_0$): The coupling saturates, $\alpha_{\text{eff}} \approx \alpha$, and the quantized increments $\Delta\Lambda = H_q \nu_h$ govern the interface evolution. This is the setting in which the distinctive HDIF predictions—horizon memory accumulation, curvature stepping, and the formation of stabilized remnants—become operative.

Implications for observational constraints. Because α_{eff} vanishes in low-curvature propagation regimes, existing gravitational-wave constraints (e.g. from LIGO/Virgo) do not restrict the fundamental coupling α . The near-vacuum environment of interferometric arms corresponds to $|R|/\Lambda_0 \ll 1$, ensuring $\alpha_{\text{eff}} \approx 0$. By contrast, the horizon-scale predictions tested in Section 7 and Section 8 operate in the fully activated regime in which $\alpha_{\text{eff}} \approx \alpha$.

This curvature-threshold structure makes explicit the behavior already encoded implicitly by the HDIF postulates: the memory kernel modifies curvature evolution only when the interface is dynamically strained, and otherwise the theory reduces exactly to general relativity in weakly-curved regions.

6.3 Macro-to-Micro Curvature Coupling and the HDIF Kernel

Einstein’s equivalence principle is often illustrated by the thought experiment of a person in free fall, for whom the effects of gravity become locally indistinguishable from uniform acceleration. In Horizons-as-Dimensional-Interface Framework (HDIF), this scenario is revisited as a concrete example of how curvature–memory coupling links astronomical and terrestrial scales. The same geometric feedback

that governs gravitational-wave dispersion (Section 6.1) also manifests, in principle, in the quasi-static Sun–Earth–observer system: the macro-scale curvature field, the planetary stress-energy distribution, and the local inertial frame of the falling body are treated as coupled components of a single interface field.

By analyzing this system across scales—from solar curvature through terrestrial gravity to the instantaneous free fall of the observer—we obtain an intuitive and experimentally accessible reconciliation between macroscopic curvature and the baseline offset Λ_0 that defines the HDIF horizon memory kernel. The following formulation translates this correspondence into measurable quantities.

1. Gravitational Field Across Scales. At the macro level, the Sun–Earth system establishes a composite potential

$$\Phi(\mathbf{r}, t) \approx -\frac{GM_\oplus}{r} + \Phi_{\text{tide}}^\odot(\mathbf{r}, t) + \Phi_{\text{tide}}^\oplus(\mathbf{r}, t) - \frac{1}{2}\omega_\oplus^2 R_\oplus^2 \cos^2\varphi \quad (43)$$

where the final term represents the centrifugal potential from Earth’s spin. The measurable local field is

$$\mathbf{g}(\mathbf{r}, t) = -\nabla\Phi(\mathbf{r}, t) \quad (44)$$

and its curvature gradient is captured by the *tidal tensor*

$$E_{ij} \equiv \partial_i \partial_j \Phi = R_{0i0j} \quad (45)$$

which represents the electric part of the Riemann tensor in general relativity. This tensor quantifies how cosmic curvature manifests as local stretching or compression—for example, in the separation of two nearby freely falling objects.

2. The Falling Man and Local Free Fall. Near Earth’s surface, an observer in free fall follows an approximate geodesic with acceleration magnitude

$$|\mathbf{g}| \approx 9.8 \text{ m/s}^2 \quad (46)$$

as measured relative to the surface. In uniform fields, the center of gravity and center of mass coincide; any small torque aligning the body arises primarily from aerodynamic effects rather than from gravity gradients. Nevertheless, the local curvature encoded in E_{ij} links the human-scale experience of fall to the astronomical curvature field. Deviations from uniform curvature can thus be modeled as a relaxation process, where the local curvature field acts as the restoring driver for memory dissipation.

For small perturbations, the relaxation time of the interface depends on the local tidal curvature amplitude. A first-order model expresses the memory kernel as

$$K(t - \tau) = K_0 \exp\left[-\frac{t - \tau}{\tau_{\text{relax}}(E_{ij})}\right] \quad (47)$$

$$\tau_{\text{relax}}(E_{ij}) = \tau_0 \left(1 + \beta \frac{|E_{ij}|}{E_\oplus}\right)^{-1} \quad (48)$$

where E_{\oplus} is a reference tidal-field strength (e.g., Earth’s surface value) and β is a dimensionless coupling factor that quantifies how strongly local tidal gradients shorten the memory-relaxation time. This form makes explicit that the curvature-memory kernel responds more rapidly in regions of stronger tidal stress, linking E_{ij} , $K(t - \tau)$, and $g_{\text{eff}}(t)$ through a measurable causal dependence.

3. HDIF Baseline and Memory Coupling. Within HDIF, the baseline horizon offset Λ_0 defines the equilibrium curvature–tension state of the interface. Deviations from this baseline—whether driven by planetary tides or subatomic curvature oscillations—produce measurable effects through a causal memory kernel:

$$\mathbf{g}_{\text{eff}}(t) = \mathbf{g}_0(t) + \int_{-\infty}^t \mathbf{K}(t - \tau) \boldsymbol{\kappa}(\tau) d\tau \quad (49)$$

where $\mathbf{g}_0(t)$ is the instantaneous gravitational field, $\boldsymbol{\kappa}(t)$ is a curvature-tension measure derived from E_{ij} , and $\mathbf{K}(t - \tau)$ is the HDIF memory kernel describing delayed relaxation of the interface. This causal relation unifies macro-scale curvature dynamics and micro-scale inertial response, tracing the interface backbone—the baseline curvature Λ_0 —from subatomic to astronomical scales.

4. Experimental Outlook. Tests of the HDIF kernel may include:

- gravimeter measurements of post-seismic or hydrological relaxation beyond elastic rebound predictions;
- drop-tower tracking of gravity-gradient variations (E_{ij}) between nearby test masses;
- high-precision $g(\varphi, t)$ measurements detecting potential phase lags relative to tidal forcing.

Detecting a reproducible hysteresis or phase-lag signature would constitute empirical evidence of curvature–memory coupling within HDIF.

For representative parameters $\nu_h = 100$ Hz and $\alpha\tau \sim 10^{-3}$, the model yields a predicted interferometric phase lag of $\Delta\phi \simeq 1.6 \times 10^{-5}$ rad. This value lies within the prospective sensitivity range of next-generation optical and gravitational-wave interferometers, providing a concrete falsifiable benchmark for HDIF’s curvature–memory coupling.

Thus, the macro-to-micro argument provides conceptual motivation for the HDIF memory kernel; the quantitative development of the framework is introduced in the following sections.

6.4 Horizon Acceleration Equation

$$a^2 = c^4 (\Lambda - \Lambda_0) = c^4 H_q \nu_h \quad (50)$$

Horizon Acceleration Equation. The structural speed limit c^2 defines the universal conversion between temporal and spatial curvature. When the local curvature Λ equals its equilibrium offset Λ_0 , the frame is inertial ($a = 0$). Departures from equilibrium generate proper acceleration, quantized through horizon oscillation frequency ν_h and coupling constant H_q .

Figure 3: **Relation between structural speed limit, curvature, and acceleration.** The baseline curvature–memory offset Λ_0 defines the inertial state. Local accelerations arise from quantized curvature deviations $\Delta\Lambda = H_q \nu_h$, with c^2 setting the maximal rate of time–space conversion across the interface. *Quantitative note:* For illustration, a representative horizon oscillation frequency $\nu_h \sim 10^{-14} \text{ s}^{-1}$ and coupling $H_q \sim 1$ yield a curvature increment $\Delta\Lambda \sim 10^{-52} \text{ m}^{-2}$, corresponding to a proper acceleration of order $a \sim 10^{-9} \text{ m/s}^2$ via Eq. (50). These values are illustrative benchmarks rather than detector-calibrated measurements.

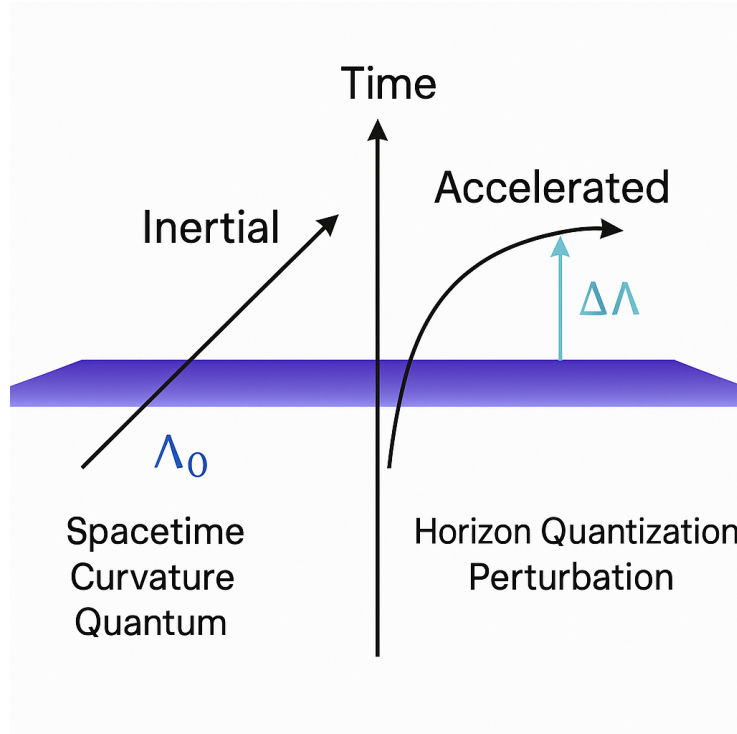


Figure 4: **Inertial vs. Accelerated Worldlines in GR and HDIF.** The left trajectory represents an inertial frame ($a = 0$), corresponding to the baseline curvature Λ_0 . The right trajectory represents a quantized acceleration state, where the curvature increases by $\Delta\Lambda = H_q\nu_h$. The structural constant c^2 governs the conversion between curvature and acceleration, linking GR's smooth geodesics to HDIF's quantized curvature-memory dynamics.

Remnant-scale observational signatures. The quantized curvature rule developed in HDIF implies that black hole evaporation cannot proceed continuously to zero curvature. Instead, evaporation halts once the interface reaches the minimum admissible curvature step, producing a stable remnant. This prediction introduces several new observational avenues. First, sub-solar or asteroid-mass compact objects that fail to follow the expected Hawking luminosity scaling would serve as direct evidence of a terminal curvature floor. Second, a population of long-lived, Planck-suppressed remnants could contribute to unexplained compact dark-matter candidates, producing microlensing signatures distinguishable from MACHOs or primordial black holes. Finally, interferometric measurements of strong-field curvature near horizon-scale objects may reveal step-wise curvature plateaus or reduced evaporation rates consistent with HDIF’s quantized horizon evolution. Together, these signatures provide an experimentally accessible path to testing the remnant prediction unique to HDIF.

Comparison with existing experimental constraints

Current precision tests of general relativity—including LIGO/Virgo gravitational-wave propagation limits, binary pulsar timing, and laboratory tests of the inverse-square law—place strong bounds on dispersion and frequency-dependent modifications to gravitational-wave signals. These analyses typically assume a modified dispersion relation of the form

$$\omega^2 = c^2 k^2 + \delta(\omega, k), \quad (51)$$

where $\delta(\omega, k)$ produces a small frequency-dependent correction to the general-relativistic group velocity. Null results from LIGO/Virgo constrain such dispersion corrections at the level $|\Delta v/c| \lesssim 10^{-15}$ across the LIGO band.

In the linearized HDIF framework, the interface field obeys a modified wave equation of the schematic form

$$[-\omega^2 + c^2 k^2] h_{ij} + i\omega \tilde{K}_C(\omega) h_{ij} + \tilde{\Sigma}_R(\omega, k) h_{ij} = 0, \quad (52)$$

leading to an effective dispersion relation

$$\omega^2 = c^2 k^2 + i\omega \tilde{K}_C(\omega) + \tilde{\Sigma}_R(\omega, k). \quad (53)$$

Naively interpreting Eq. (53) as a homogeneous modification to gravitational-wave propagation suggests that the phenomenological parameters $(\alpha, \tau, \kappa_{\text{mem}})$ are strongly constrained: for characteristic frequencies in the LIGO band ($f \sim 10\text{--}10^3$ Hz) and illustrative values $\alpha \sim 0.1\text{--}1$, $\tau \sim 10^{-3}$ s, the induced group-velocity shift $\Delta v/c$ would generically be of order α times a function of $\omega\tau$ that is not parametrically suppressed. A direct application of the LIGO/Virgo bound $|\Delta v/c| \lesssim 10^{-15}$ would then appear to push α to extremely small values, in obvious tension with the fiducial order-unity range used elsewhere in this paper.

At present we regard this as an indication that the simple, homogeneous plane-wave treatment of Eq. (53) is incomplete rather than as a decisive exclusion of the HDIF parameter space. In particular, the curvature-memory kernel

in HDIF is intended to be strongest near high-curvature interfaces (horizons, Casimir-like boundaries, or strongly strained media), whereas the LIGO constraints are derived from gravitational-wave propagation through very weakly curved, effectively vacuum regions. A fully covariant treatment of how the HDIF memory kernel couples to different background curvatures is required before robust constraints can be extracted. Until such an analysis is performed, the $(\alpha, \tau, \kappa_{\text{mem}})$ values quoted in this work should be viewed as phenomenological benchmarks illustrating the possible size of curvature–memory effects, rather than as parameter choices demonstrably compatible with all existing gravitational-wave bounds.

Resolving this apparent tension between illustrative HDIF parameter choices and gravitational-wave dispersion bounds is a priority for future work.

7 Horizon Quantization and Scaling Relations

Here, ‘field structure’ refers specifically to the GR-compatible, coarse-grained representation introduced in the Master Field Formula Eq. (24).

Baseline Definitions.

$$\begin{aligned}
\ell_P &= \sqrt{\frac{\hbar G}{c^3}} && \text{(Planck length)} \\
t_P &= \sqrt{\frac{\hbar G}{c^5}} && \text{(Planck time)} \\
\Lambda_P &\equiv \ell_P^{-2} && \text{(Planck curvature scale)} \\
\Lambda_0 &&& \text{(HDIF baseline coherence offset)} \\
\eta &\equiv \frac{\Lambda_0}{\Lambda_P} && \text{(dimensionless ratio)}
\end{aligned}$$

Memory–kernel factor: $\kappa_m \in (0, 1]$ encodes the kernel’s effective stiffness or shape.

Definition (units check: H_q **has** s m^{-2} **).**

$$\boxed{H_q \equiv \kappa_m \eta \frac{t_P}{\ell_P^2} = \kappa_m \frac{\Lambda_0}{\Lambda_P} \frac{t_P}{\ell_P^2}} \tag{54}$$

Memory Operator. HDIF models curvature–memory feedback through a linear integral operator,

$$L_{\text{mem}}[X](t) = \int_0^\infty K(\tau) X(t - \tau) d\tau \tag{55}$$

where $K(\tau)$ is the system’s memory kernel. This operator acts on geometric quantities such as curvature increments or tension variations and governs the rate at which past states influence the present curvature response.

Horizon Memory Timescale. The characteristic horizon memory timescale is defined by

$$\tau_h = \frac{\int_0^\infty \tau K(\tau) d\tau}{\int_0^\infty K(\tau) d\tau} \quad (56)$$

which represents the effective duration over which past curvature states significantly contribute to the present horizon response.

Horizon Response Frequency. The corresponding horizon response frequency is

$$\nu_h = \tau_h^{-1} \quad (57)$$

which sets the rate at which curvature-memory feedback equilibrates at a horizon boundary.

While the quantization condition introduced below mirrors atomic energy levels, its origin here is geometric: the memory-coupled curvature field satisfies an eigenvalue problem for the operator $\mathcal{L}_{\text{mem}} = \square + \alpha \int K(t-t') (\cdot) dt'$. Boundary regularity at the horizon enforces discrete eigenfrequencies ν_h whose corresponding curvature increments $\Delta\Lambda$ satisfy Eq. (58). Thus the quantization of curvature arises from boundary-value conditions on the memory operator, not from analogy alone.

Quantization Rule for Horizon States.

$$\boxed{\Delta\Lambda = H_q \nu_h} \quad (58)$$

where ν_h is the interface's curvature-memory oscillation frequency. Interpretation: a horizon's allowed "steps" in curvature are quantized by the coherence quantum H_q times its interface oscillation rate.

Alternative Planck-unit form.

$$H_q = \kappa_m \eta \frac{t_P}{\ell_P^2} = \kappa_m \eta (\ell_P^{-2} t_P)$$

This formulation ties discrete horizon shifts to **coherence (memory) + curvature**, rather than to action alone.

Numerical Sanity Check (Representative Values). Using $\ell_P \approx 1.616255 \times 10^{-35} \text{ m}$, $t_P \approx 5.391247 \times 10^{-44} \text{ s}$, $\Lambda_P = \ell_P^{-2} \approx 3.83 \times 10^{69} \text{ m}^{-2}$, and $\Lambda_0 \approx 1.11 \times 10^{-52} \text{ m}^{-2}$, we find:

$$\eta = \frac{\Lambda_0}{\Lambda_P} \approx 2.89 \times 10^{-122}$$

$$H_q(\kappa_m=1) \approx 5.96 \times 10^{-96} \text{ s m}^{-2}$$

Representative horizon states:

$$\begin{aligned}
\nu_h \sim 10^3 \text{ Hz} &\Rightarrow \Delta\Lambda \sim 6 \times 10^{-93} \text{ m}^{-2} && (\text{stellar BH ringdown}) \\
\nu_h \sim 10^{-3} \text{ Hz} &\Rightarrow \Delta\Lambda \sim 6 \times 10^{-99} \text{ m}^{-2} && (\text{SMBH ringdown}) \\
\nu_h \sim 10^{-18} \text{ Hz} &\Rightarrow \Delta\Lambda \sim 6 \times 10^{-114} \text{ m}^{-2} && (\text{cosmic horizon})
\end{aligned}$$

Interpretation. These values are extremely small—as expected—because the observed Λ_0 is roughly 10^{-122} of the Planck curvature. If HDIF predicts locally enhanced Λ_0 near strong horizons, η and thus H_q scale upward accordingly.

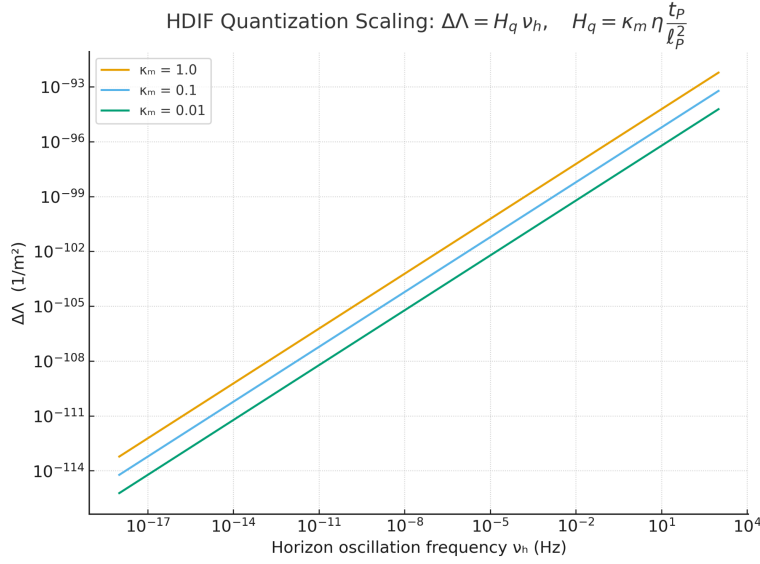


Figure 5: Quantized curvature increment $\Delta\Lambda = H_q \nu_h$ predicted by HDIF as a function of horizon-oscillation frequency ν_h . Curves correspond to three representative memory-coupling strengths $\kappa_{\text{mem}} = 1, 0.1, 0.01$ in the expression $H_q = \kappa_{\text{mem}} \eta t_P / \ell_P^2$. The shaded observationally relevant band (10^{-52} m^{-2}) marks the curvature scale associated with cosmic acceleration. Frequencies to the left of $\nu_h \lesssim 10^{-14} \text{ Hz}$ correspond to cosmological-timescale modes, whereas higher values ($10^{-3} \text{--} 10^2 \text{ Hz}$) fall into the interferometric detection band. This figure illustrates how HDIF’s quantization rule connects memory coupling, curvature increments, and possible observable signatures across different frequency regimes.

Figure 5 places the HDIF quantization rule $\Delta\Lambda = H_q \nu_h$ into an observational context. For $\kappa_{\text{mem}} \sim 0.1\text{--}1$, the predicted curvature steps span $\Delta\Lambda \sim 10^{-114}\text{--}10^{-52} \text{ m}^{-2}$ across the frequency range $10^{-17}\text{--}10^4 \text{ Hz}$. The upper end of this range intersects the curvature scale associated with cosmic acceleration ($\sim 10^{-52} \text{ m}^{-2}$), while lower frequencies correspond to extremely slow horizon-memory modes that would manifest only in long-timescale residual

curvature offsets. Thus the scaling in Fig. 5 identifies which combinations of κ_{mem} and ν_h are observationally relevant and which lie far below measurable thresholds.

Physical Meaning and HDIF Connection. In the Horizons-as-Dimensional-Interface Framework (HDIF), horizons are not fixed geometric boundaries but *memory-bearing surfaces* whose curvature evolves in discrete steps determined by their stored tension history. The parameter H_q therefore plays an analogous role to Planck’s constant in quantum mechanics—it defines the smallest measurable “unit” of curvature–memory exchange within an interface.

While Planck’s constant quantizes *action*, H_q quantizes *geometric response*: it governs how curvature can adjust when a horizon’s memory kernel releases or absorbs tension. The ratio $\eta = \Lambda_0/\Lambda_P$ expresses how far the present universe lies below the Planck curvature scale, and the kernel factor κ_m introduces the local stiffness or coherence of the interface. Together these determine the effective “grain” of curvature evolution at any scale.

In this view, Eq. (58)

$$\Delta\Lambda = H_q \nu_h$$

links **temporal coherence** (ν_h , the oscillation frequency of the interface) to **spatial curvature increments** ($\Delta\Lambda$), showing that a horizon’s curvature cannot vary continuously but in discrete packets proportional to its internal oscillation mode. When the memory kernel is stiff ($\kappa_m \rightarrow 1$), curvature steps are large; when memory is compliant, curvature changes occur in finer increments. These relations embed horizon quantization directly into the broader Horizons-as-Dimensional-Interface framework:

- the **memory term** connects to the damping tensors $C_{\mu\nu}$ in Eq. (21).
- the **curvature increment** $\Delta\Lambda$ reflects the residual entanglement curvature $R_{\mu\nu}$ Eq. (22).
- the **baseline offset** Λ_0 ties back to the cosmological coherence offset introduced in Section 3.4.

Consequently, the horizon quantization condition acts as the microscopic closure rule for the entire theory, ensuring that global curvature (cosmic acceleration) and local oscillatory phenomena (ringdown, interferometric phase lags) emerge from the same quantized interface mechanics².

7.1 Relation to existing modified-gravity models

To situate HDIF within the broader landscape of modified-gravity research, it is useful to contrast its field structure with three major approaches: $f(R)$ extensions, scalar–tensor theories, and entropic-gravity models.

²Note that κ_m is a *dimensionless* stiffness factor normalized to unity; it does not carry the physical units of H_q . The limit $\kappa_m \rightarrow 1$ represents maximal curvature–memory coupling (perfect coherence), not a dimensional bound such as $1 \text{ m}^2/\text{s}$.

$f(R)$ gravity. In $f(R)$ theories, the Einstein–Hilbert action $S = \int \sqrt{-g} R$ is replaced by a nonlinear function $f(R)$ [28, 29], leading to modified field equations

$$f'(R) R_{\mu\nu} - \frac{1}{2} f(R) g_{\mu\nu} + (g_{\mu\nu} \square - \nabla_\mu \nabla_\nu) f'(R) = 8\pi G T_{\mu\nu} \quad (59)$$

These models re-weight the local curvature response through derivatives of R . By contrast, HDIF preserves the linear Einstein tensor form but introduces a convolutional memory term, $C_{\mu\nu} = \int K_C(x, x') \Xi_{\mu\nu}(x') d\mu(x')$, representing a *nonlocal time-dependent* weighting of curvature. Thus, rather than modifying the function of R , HDIF generalizes its temporal response through memory kernels.

Scalar–tensor theories. Scalar–tensor models such as Brans–Dicke theory [30] introduce an additional scalar field ϕ that modulates the effective gravitational constant [31], leading to $G_{\mu\nu} = 8\pi G T_{\mu\nu}/\phi$ and a companion field equation for ϕ . HDIF differs conceptually in that no new scalar field is postulated; instead, curvature feedback is governed by the causal kernel $K(t - t')$, which plays the role of a *distributed susceptibility*. The resulting memory coupling $\alpha \int K(t - t') \dot{\kappa}(t') dt'$ produces effective delays similar to scalar backreaction, but without an independent field degree of freedom.

Entropic and emergent-gravity models. Entropic-gravity frameworks [32, 33] interpret gravity as an emergent thermodynamic phenomenon arising from horizon information content, but lack an explicit dynamical mechanism for how horizon microstates produce curvature response. HDIF complements these models by supplying a geometric memory kernel that links entropy flow to measurable curvature lag, thereby providing a concrete differential operator for the thermodynamic analogy.

In summary, whereas $f(R)$ and scalar–tensor models [34] modify or augment the field content of general relativity, HDIF retains Einstein’s local form and extends it through nonlocal, causal memory coupling. This allows curvature, tension, and information flow to coexist within a unified geometric framework that remains falsifiable through phase-lag and Casimir-scale experiments.

7.2 HDIF Horizon Quantization Condition (atomic analogue)

$$\iint_{\Sigma} \kappa_M d\Sigma = N_H \Lambda_0 \quad (60)$$

$$\oint_{\gamma} \mathbf{T}_{\text{int}} \cdot d\boldsymbol{\ell} = 2\pi N_H \Lambda_0 \quad (61)$$

$$\oint_{\gamma} \nabla \phi_H \cdot d\boldsymbol{\ell} = 2\pi N_H \iff N_{\text{nodes}} = N_H - \ell - 1 \quad (62)$$

Where:

$N_H \in \mathbb{Z}_{\geq 0}$ — horizon/level index (HDIF analogue of principal quantum number)

Λ_0 — horizon quantization constant (unit of curvature–memory flux)

$\kappa_M(t) = \int_0^\infty K(\tau) \kappa(t-\tau) d\tau$ — curvature κ weighted by causal memory kernel $K(\tau)$

$\mathbf{T}_{\text{int}} \propto \nabla \cdot \kappa_M$ — interface tension 1-form sourcing the loop condition

ϕ_H — interface phase, defined by $\kappa_M = |\kappa_M| e^{i\phi_H}$

$N_{\text{nodes}} = N_H - \ell - 1$ — radial node count, mirroring atomic shell structure

The quantized increments of curvature described above imply that information flow across horizons must carry a measurable entropic imprint. We now formalize this relationship between entropy, holographic area, and curvature-memory diffusion.

7.3 Entropy and Memory Coupling Across Horizons

Entropy increase corresponds to the widening of the memory kernel, reflecting a reduction in curvature–memory coherence. In statistical mechanics, the entropy of a macroscopic configuration is given by

$$S = k_B \ln \Omega \quad (63)$$

where Ω is the number of microscopic configurations (microstates) consistent with the same observable macrostate. The second law then arises statistically: systems evolve toward configurations with overwhelmingly greater Ω , corresponding to higher entropy. In such formulations, individual microstates are typically assumed to be independent and memoryless.

In HDIF, each curvature configuration of spacetime constitutes a *memory-coupled macrostate*, in which the local curvature field $\Lambda(t)$ retains a continuous dependence on its preceding history. The dynamical evolution is expressed as

$$\Lambda(t) = \Lambda_0 + \int_{-\infty}^t K(t-t') \dot{\Lambda}(t') dt' \quad (64)$$

where $K(t-t')$ is a memory kernel describing the delayed response of curvature to prior curvature change. Rather than independent microstates, HDIF therefore describes a continuum of *microhistories*, each weighted by its contribution to the present curvature through $K(t-t')$.

This memory dependence reframes entropy not as ignorance of microstates, but as the cumulative measure of *damped coherence* across curvature histories. As curvature-memory correlations diffuse over time, the effective entropy increases:

$$\frac{dS}{dt} \propto - \frac{d}{dt} \left[\int_{-\infty}^t |K(t-t')|^2 dt' \right] \quad (65)$$

where the negative sign reflects the convention that entropy increases as the kernel norm decreases; a narrower kernel corresponds to lower curvature–memory coherence, consistent with increasing statistical degeneracy. This process represents a gradual redistribution of coherence into statistical degrees of freedom.

In the holographic limit, the boundary area A of a horizon encodes the system’s information capacity,

$$S_{\text{holo}} = \frac{k_B A}{4 \ell_P^2} \quad (66)$$

and in HDIF this boundary acts as a *memory surface* recording the integrated curvature history of the enclosed region. The approach to equilibrium corresponds to the broadening of the kernel $K(t - t')$ —a geometric analogue of the mixing of microstates in thermodynamics.

Hence, the apparent probabilistic behavior of entropic systems is modeled as arising from path-dependent determinism: as curvature–memory coherence decreases, the system becomes compatible with a broader ensemble of admissible geometric configurations. Entropy, in this framework, corresponds to the degree of diffusion of curvature-memory across the horizon interface as the memory kernel widens.

7.4 Reference, Memory, and Probabilistic Amplitudes

In HDIF, probabilistic amplitudes can be represented as effective descriptions of curvature–memory damping, without assigning any ontological randomness to spacetime itself.

In classical physics, determinism arises because all dynamical variables are defined with respect to well-defined reference frames. Trajectories, accelerations, and energies are meaningful only insofar as they are compared against an external continuum of coordinates that provides temporal and spatial context. Once this continuum of references is lost—when a subsystem becomes isolated from macroscopic clocks or rulers—its internal evolution can only be expressed relationally. The absence of absolute references means that a subsystem’s evolution can only be described in terms of relative configurations, for which probabilistic amplitudes can be used as effective representations of incomplete reference information.

Quantum theory captures this condition through the state function $\psi(x, t)$, whose squared amplitude $|\psi|^2$ yields statistical outcomes. The probabilistic character of measurement thus reflects not intrinsic indeterminacy but the loss of referential coherence: the system’s history can no longer be traced to a continuous external record.

Within HDIF, this statistical behavior emerges naturally from the *memory-damping* of curvature coherence. Each local horizon patch retains only a partial record of past curvature through its causal memory kernel $K(t - t')$. When K maintains long-range correlation, the curvature field evolves deterministically.

As the kernel decays and historical links are erased, the interface's future state becomes expressible only as a weighted ensemble of possible continuations:

$$P(\Lambda, t) \propto \int \exp\left[-\frac{1}{2\sigma^2} \int |K(t-t')|^2 dt'\right] d(\text{histories}) \quad (67)$$

The Gaussian weighting in Eq. (67) arises naturally from the central-limit behavior of cumulative curvature fluctuations. If the fluctuations around the mean memory trajectory are treated as small, approximately independent perturbations δK_i with variance σ^2 , the total memory deviation $\sum_i \delta K_i$ converges toward a normal distribution by the law of large numbers. The long-range correlations encoded in $K(t-t')$ remain intact; only the stochastic deviations about the mean contribute to the Gaussian weighting. Consequently, the probability of a given curvature-history path is weighted by the exponential factor shown above, representing the most likely ensemble of memory-damped trajectories.

Here σ^2 represents the variance of curvature-memory fluctuations per causal interval; empirically, it sets the scale of decoherence between successive reference-preserving states. In this first formulation, σ^2 is treated as a phenomenological constant to be determined experimentally or from a future microscopic model of curvature fluctuations. Thus, HDIF models probabilistic weighting as an effective description of memory-retention limits, set by the empirically determined decoherence scale σ^2 , without invoking any additional quantum postulate. In this sense, within HDIF, probabilistic weights reflect incomplete retention of curvature-memory information rather than any intrinsic randomness of spacetime.

As a simple illustration, one may consider two curvature modes with memory kernels $K_1, K_2 \approx e^{-t/\tau_{1,2}}$, for which $\int |K_i|^2 dt = \frac{1}{2}\tau_i$. Substituting this into Eq. (62) gives

$$\frac{P_1}{P_2} = \exp\left[-\frac{\tau_1^2 - \tau_2^2}{2\sigma^2}\right] \quad (68)$$

which reproduces a Boltzmann-like weighting expected from entropic diffusion. This example demonstrates that even simplified memory kernels yield probability ratios consistent with thermodynamic expectations, thereby linking curvature-memory damping to statistical irreversibility. Thus, within the HDIF model, probabilistic weights can be represented as arising from incomplete retention of curvature-memory information, linking memory damping to behavior consistent with statistical irreversibility. In this sense, HDIF models probabilistic outcomes as reflecting the degree to which past curvature states are only partially encoded in the present interface.

In this picture, HDIF interpolates between coherent geometric evolution and effectively statistical behavior as the memory kernel decays. When curvature-memory coherence is high, the interface dynamics retain detailed information about prior curvature states; as coherence decreases through damping, the evolution becomes increasingly consistent with statistical irreversibility. In this framework, probabilistic behavior is associated with the degree of diffusion of curvature-memory across the horizon interface.

The synthesis of determinism and probability through curvature–memory dynamics aligns naturally with prior thermodynamic and holographic treatments of gravity. Where Jacobson [35] derived the Einstein equations from thermodynamic identities and Verlinde [33] framed gravity as an entropic force associated with information gradients, HDIF extends these ideas by linking entropy production and probabilistic weighting to the diffusion of geometric memory through the explicit memory kernels appearing in the field equations. Section 9 situates this interpretation in relation to those antecedent frameworks and clarifies how HDIF’s memory kernels provide a concrete, dynamical mechanism underlying their statistical analogues.

From quantized curvature to evaporation. The quantization rule for horizon curvature obtained in this section, $\Delta\Lambda = H_q\nu_h$, establishes that interface evolution cannot proceed through arbitrarily small changes in curvature. Any horizon subject to HDIF dynamics must therefore evolve through discrete curvature steps, with a lower bound set by the smallest admissible increment. In the next section we apply this structure to Hawking evaporation, showing that the discrete curvature ladder implied by HDIF prevents complete evaporation and instead drives black holes toward stable remnant states with non-zero terminal curvature.

8 Black Hole Remnants in HDIF: Quantized Evaporation and Irreducible Curvature States

In the Horizons-as-Dimensional-Interface Framework (HDIF), horizons are memory-bearing curvature interfaces whose evolution proceeds through discrete increments. This follows from the quantization rule Eq. (58):

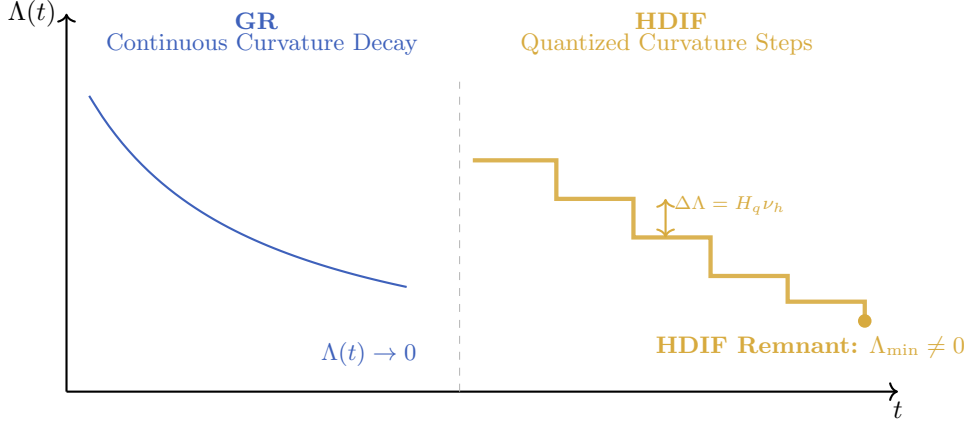
$$\Delta\Lambda = H_q\nu_h$$

derived in Section 7, where H_q is the coherence–curvature coupling constant and ν_h is the interface’s oscillation frequency. Because curvature cannot vary continuously, the evaporation of a black hole through Hawking radiation cannot proceed to zero horizon area or zero mass. Instead, the shrinkage of the horizon terminates when the curvature reaches the smallest permissible step.

8.1 Quantized Evaporation and the Terminal Horizon State

In semiclassical gravity [36, 37], Hawking radiation predicts that a black hole of initial mass M loses mass continuously until the horizon radius $r_h = 2GM/c^2$ vanishes. HDIF alters this picture fundamentally. Since curvature changes only in discrete increments $\Delta\Lambda$, the approach to zero area is halted once the remaining curvature is within one quantum step of the baseline value Λ_0 . At this point,

the interface cannot shed additional curvature without violating the quantized evolution rule Eq. (58), so the evaporation process stalls.



This final object is a *black hole remnant*: a stable, non-zero-area interface configuration whose curvature and mass lie at the lower bound permitted by HDIF's quantization structure. The remnant is characterized by

$$\Lambda_{\text{rem}} - \Lambda_0 \sim \Delta\Lambda_{\text{min}} = H_q \nu_{h,\text{min}} \quad (69)$$

where $\nu_{h,\text{min}}$ is the smallest sustained oscillation mode the interface can support without decoherence. The horizon's geometric memory kernel prevents further collapse, enforcing a non-zero terminal mass M_{rem} .

8.2 Memory Conservation and the Information Paradox

Black hole remnants provide a natural resolution to the information paradox. HDIF distinguishes between *weak-reference memory*, which decays through Hawking radiation, and *strong-reference memory*, which is stored in the curvature coherence of the horizon interface. The strong-reference component cannot evaporate, because eliminating it would require curvature shifts smaller than the quantum increment $\Delta\Lambda_{\text{min}}$.

Thus the remnant acts as a carrier of irreducible geometric memory:

- weak-reference memory \rightarrow radiated as Hawking modes.
- strong-reference memory \rightarrow preserved in the remnant.

No information is destroyed; it is redistributed between decoherent radiation channels and a stable core containing the minimal curvature signature consistent with HDIF.

8.3 Cosmological Implications of HDIF Remnants

If black holes cannot evaporate fully, the universe must accumulate a population of curvature remnants over cosmic time. Each remnant is a stable, Planck-

suppressed, low-radius interface structure whose mass is small but non-zero. HDIF therefore predicts:

1. the existence of long-lived remnant populations following each astrophysical black hole’s evaporation epoch,
2. a non-negligible contribution of remnants to dark matter-like gravitational effects,
3. cosmological memory retention through these stable cores.

Since each remnant carries the strongest surviving curvature-memory reference of its progenitor, the late-time universe retains a “compressed record” of high-curvature events. This memory cannot be erased without violating HDIF’s quantization rules.

8.4 Terminal Geometry and the End-State of the Universe

The existence of irreducible curvature states at horizon boundaries implies a broader cosmological consequence: the universe itself cannot decay to an exactly flat or empty geometry. Just as black hole evaporation halts at the minimum curvature increment, cosmic expansion cannot erase curvature beyond the smallest interface quantum.

This frames the ultimate end-state of the universe as a finite, memory-saturated configuration composed of:

- a cold radiation background carrying weak-reference memory.
- a population of quantized curvature remnants preserving strong-reference memory.
- a residual coherence offset Λ_0 representing the minimum curvature-memory density of spacetime.

HDIF therefore predicts that the universe does not evolve toward an exactly empty, flat, and zero-temperature state. Instead, it asymptotically approaches a stable interface configuration defined by the same quantized curvature principles governing black hole remnants.

8.5 Summary

Within HDIF, black hole remnants are not an optional extension of the theory but a *necessary consequence* of curvature quantization. Since curvature-memory interfaces cannot evolve continuously, Hawking evaporation terminates at the smallest admissible curvature increment. These remnants resolve the information paradox, contribute to dark matter-like structure, and define the universe’s non-vanishing terminal geometry. The same interface principles that quantize curvature locally also shape the global fate of cosmic evolution.

9 Connections to Literature

The Horizons-as-Dimensional-Interface Framework (HDIF) builds upon and extends several foundational approaches aimed at reconciling general relativity (GR) and quantum field theory (QFT), particularly those framing gravity as emergent from microscopic degrees of freedom. The modern ‘islands’ program further supports horizon-centric mechanisms for information flow.

Jacobson [35] derived the Einstein field equations from the thermodynamic identity $\delta Q = TdS$ applied to local Rindler horizons, suggesting that curvature can be understood as a macroscopic equation of state. This thermodynamic perspective spurred numerous horizon-based models in which gravity emerges from statistical mechanics of underlying microstates.

Verlinde [33] proposed that gravity arises as an entropic force associated with information changes on holographic screens, while Bousso’s covariant entropy bounds [12] and Susskind’s holographic principle [13] formalized the idea that boundaries encode bulk physics.

HDIF extends these frameworks by adding a *curvature–memory coupling* absent from previous emergent-gravity models. In this view, horizons are modeled as boundary surfaces with effective memory kernels, which capture the influence of past curvature states on present dynamics. This storage is formalized via *integral memory kernels* that directly enter the field equations, producing measurable phase lags, oscillatory shear, and quantized deviations in geodesic behavior near high-coherence boundaries.

Unlike Jacobson and Verlinde, who emphasize entropy gradients or bulk–boundary thermodynamics, HDIF treats space and matter as two excitation modes of the same interface geometry. We model space as the baseline (equilibrium) solution of the interface equations, and matter as localized perturbations of that baseline. Thus, space and matter are treated as coupled excitation modes of the same interface geometry, making curvature–memory feedback physically inevitable: any change in one necessarily modifies the other.

While entropy-based approaches often remain statistical, HDIF’s formulation is explicitly dynamical. The interface curvature tensor incorporates measurable quantities such as:

- Horizon tension gradients $\delta\kappa(I)$
- Scalar–tension mismatch $\Theta_{\mu\nu}$
- Residual entanglement curvature $\mathcal{R}_{\mu\nu}$

Each appears in falsifiable predictions, including discrete shear steps in gravitational lensing and phase-delayed curvature shifts in gravitational wave interferometry [14, 15, 25, 27].

In summary, HDIF draws conceptual lineage from Jacobson’s thermodynamic horizon, Verlinde’s entropic gravity, and holographic bounds, but advances them by embedding memory as a geometric degree of freedom within postulate-driven field equations derived from the Master Field Formula, yielding a mechanically

predictive and experimentally testable framework that reconciles quantum and relativistic regimes.

Connections to remnant proposals. Black hole remnants have been proposed in several contexts, including generalized uncertainty principle (GUP) models, asymptotically safe gravity, and certain approaches to loop quantum gravity. These frameworks typically invoke modifications to short-distance structure or quantum geometry to halt evaporation. HDIF differs fundamentally: remnants arise not from modified commutators or discrete geometric spectra, but from the quantized curvature response enforced by memory-coupled interface dynamics. Whereas GUP and Planck-scale discreteness impose ultraviolet cutoffs, HDIF predicts remnants as a dynamical consequence of horizon memory evolution. This places HDIF in a distinct category, providing a mechanism grounded in curvature–memory feedback rather than kinematic quantization alone, and offering a falsifiable strong-field prediction that can be contrasted with existing remnant models.

10 Conclusion & Path to Testing

The Horizons-as-Dimensional-Interface Framework (HDIF) proposes that space-time curvature, memory, and quantization arise from a single boundary-field mechanism. Within this picture, geometric curvature is not a continuously varying quantity but evolves through discrete increments driven by memory-coupled interface dynamics. This perspective unifies relativistic geometry with quantum-correlational behavior by identifying interfaces as the fundamental carriers of both curvature response and geometric memory.

A key result of HDIF is the quantization rule $\Delta\Lambda = H_q\nu_h$, which links horizon-scale curvature increments to the interface’s oscillation frequency and coherence–curvature coupling constant. This condition provides a geometric closure for HDIF: curvature cannot evolve arbitrarily, but only through discrete steps determined by the internal dynamics of the interface. The same mechanism that governs quantum correlations in weak-field contexts reappears in strong-field regimes as quantized curvature evolution.

These features mark HDIF as a falsifiable interface-based unification of GR and QFT: geometric memory, delayed curvature response, and horizon-scale quantization emerge from the same interface tensor field. The theory therefore makes distinct predictions that differentiate it from existing gravitational or quantum-gravity models. In particular, HDIF’s black-hole remnants arise from quantized curvature–memory dynamics rather than ultraviolet cutoffs or modified commutators, placing HDIF in a category distinct from GUP- or LQG-based remnant models.

Path to Testing

HDIF makes concrete, testable predictions across several observational and laboratory regimes:

- **Curvature–Memory Phase Lags:** Precision interferometry (atom interferometers, optical cavities, resonant-mass detectors) can probe delayed curvature response predicted by the horizon memory kernel $\hat{K}_C(\omega)$.
- **Quantized Lensing Signatures:** Strong-lensing environments near compact objects may exhibit micro-step deflections or mode transitions corresponding to discrete curvature increments.
- **Interference-Pattern Deviations:** In Casimir-based setups or long-baseline optical systems, HDIF predicts interference-pattern modifications generated by residual geometric memory.
- **Gravitational-Wave Phase Shifts:** In the low-frequency limit, HDIF predicts a measurable correction to gravitational-wave dispersion, encoded through the effective mass scale m_R and memory-induced damping $\hat{\Sigma}_R$.
- **Black-Hole Remnants:** HDIF predicts that Hawking evaporation stalls at a finite curvature step $\Delta\Lambda_{\min}$, yielding stable remnants with non-zero terminal mass. These provide a clear observational discriminator between HDIF, GUP, asymptotic-safety proposals, and quantum-geometry discreteness models.

Together, these predictions outline a multi-pronged strategy for empirical testing. Laboratory interferometry constrains near-horizon memory response; astronomical observations probe curvature quantization in strong fields; and gravitational-wave dispersion offers a complementary test of the interface tensor’s dynamics. HDIF is therefore positioned not merely as a conceptual framework, but as a falsifiable physical theory whose predictions can be evaluated with present or near-future experimental capabilities.

Funding

Funding information – not applicable.

Acknowledgements

The author acknowledges the use of AI-based research tools, including OpenAI’s ChatGPT and Anthropic’s Claude, for assistance in refining the manuscript’s structure, language, and presentation. Their role was advisory and reflective, not authorial.

Competing Interests

The author declares no competing interests.

References

- [1] Bekenstein, J.D.: Black holes and entropy. *Phys. Rev. D* **7**, 2333–2346 (1973)
- [2] Maldacena, J.: The large-N limit of superconformal field theories and supergravity. *Adv. Theor. Math. Phys.* **2**, 231–252 (1998)
- [3] Rovelli, C.: Relational quantum mechanics. *Int. J. Theor. Phys.* **35**, 1637–1678 (1996)
- [4] Einstein, A.: The foundation of the general theory of relativity. *Ann. Phys.* **49**, 769–822 (1916)
- [5] Israel, W.: Singular hypersurfaces and thin shells in general relativity. *Il Nuovo Cimento B* **44**, 1–14 (1966)
- [6] Poisson, E., Visser, M.: Thin-shell wormholes: Linearization stability. *Phys. Rev. D* **52**, 7318–7321 (1995)
- [7] E. Noether, Invariante Variationsprobleme, *Nachr. D. Königl. Gesellsch. D. Wiss. Göttingen, Math.-Phys. Kl.* **1918**, 235 (1918).
- [8] Bagley, R.L., Torvik, P.J.: A theoretical basis for the application of fractional calculus to viscoelasticity. *J. Rheol.* **27**, 201–210 (1983)
- [9] Mainardi, F.: Fractional relaxation–oscillation and fractional viscoelasticity. *Chaos Solitons Fractals* **7**, 1461–1477 (1996)
- [10] Maggiore, M.: Nonlocal infrared modifications of gravity: a review. *Fundam. Theor. Phys.* **187**, 221–281 (2017)
- [11] Donoghue, J.F.: Quantum gravity as a low-energy effective field theory. *Scholarpedia* **12**(4), 32997 (2017)
- [12] Bousso, R.: The holographic principle. *Rev. Mod. Phys.* **74**, 825–874 (2002)
- [13] Susskind, L.: The world as a hologram. *J. Math. Phys.* **36**, 6377–6396 (1995)
- [14] Kubo, R.: The fluctuation–dissipation theorem. *Rep. Prog. Phys.* **29**, 255–284 (1966)
- [15] Zwanzig, R.: Nonlinear generalized Langevin equations. *J. Stat. Phys.* **9**, 215–220 (1973)
- [16] Einstein, A., Podolsky, B., Rosen, N.: Can quantum-mechanical description of physical reality be considered complete? *Phys. Rev.* **47**, 777–780 (1935)
- [17] Almheiri, A., Hartman, T., Maldacena, J., Shaghoulian, E., Tajdini, A.: The entropy of Hawking radiation and the island formula. *Rev. Mod. Phys.* **93**, 035002 (2021)

- [18] Penington, G.: Entanglement wedge reconstruction and the information paradox in evaporating black holes. *J. High Energy Phys.* **2020**, 002 (2020)
- [19] Engelhardt, N., Wall, A.C.: Quantum extremal surfaces: holographic entanglement beyond the classical regime. *JHEP* **2015**, 73 (2015)
- [20] Heisenberg, W.: The physical content of quantum theoretical kinematics and mechanics. *Z. Phys.* **43**, 172–198 (1927)
- [21] Bernstein, S.: Sur les fonctions absolument monotones. *Acta Mathematica* **52**, 1–66 (1929)
- [22] Steinhauer, J.: Observation of quantum Hawking radiation and its entanglement in an analogue black hole. *Nat. Phys.* **12**, 959–965 (2016)
- [23] Weinfurtner, S., Tedford, E., Penrice, M., Unruh, W.G., Lawrence, G.A.: Measurement of stimulated Hawking radiation in an analogue system. *Nat. Phys.* **7**, 865–868 (2011)
- [24] Philbin, T.G., Kuklewicz, C., Robertson, S., Hill, S., König, F., Leonhardt, U.: Fiber-optical analogue of the event horizon. *Science* **319**, 1367–1370 (2008)
- [25] Barceló, C., Liberati, S., Visser, M.: Analogue gravity. *Living Rev. Relativ.* **14**, 3 (2011)
- [26] Leonhardt, U., Philbin, T.G.: Black hole analogues in dielectric media. *Prog. Opt.* **53**, 69–152 (2008)
- [27] Asenbaum, P., Overstreet, C., Kim, M., Curti, J., Kasevich, M.A.: Atom-interferometric test of the equivalence principle at the 10^{-12} level. *Phys. Rev. Lett.* **125**, 191101 (2020)
- [28] Sotiriou, T. P., Faraoni, V.: $f(R)$ theories of gravity. *Rev. Mod. Phys.* **82**, 451–497 (2010)
- [29] De Felice, A., Tsujikawa, S.: $f(R)$ theories. *Living Rev. Relativ.* **13**, 3 (2010)
- [30] Brans, C., Dicke, R. H.: Mach’s principle and a relativistic theory of gravitation. *Phys. Rev.* **124**, 925 (1961)
- [31] Fujii, Y., Maeda, K.: *The Scalar–Tensor Theory of Gravitation*. Cambridge University Press, Cambridge (2003)
- [32] Padmanabhan, T.: Thermodynamical aspects of gravity: New insights. *Rep. Prog. Phys.* **73**, 046901 (2010)
- [33] Verlinde, E.: On the origin of gravity and the laws of Newton. *J. High Energy Phys.* **2011**, 029 (2011)
- [34] Clifton, T., Ferreira, P. G., Padilla, A., Skordis, C.: Modified gravity and cosmology. *Phys. Rep.* **513**, 1–189 (2012)

- [35] Jacobson, T.: Thermodynamics of spacetime: The Einstein equation of state. *Phys. Rev. Lett.* **75**, 1260–1263 (1995)
- [36] Hawking, S.W.: Black hole explosions?. *Nature* **248**, 30–31 (1974)
- [37] Hawking, S.W.: Particle creation by black holes. *Commun. Math. Phys.* **43**, 199–220 (1975)

Appendix A — Kernel Admissibility Lemma

Lemma. If $K_C(\Delta\tau)$ is causal and completely monotone, then $\text{Re } \widehat{K}_C(\omega) \geq 0$ and $\widehat{K}_C(\omega)$ is analytic for $\text{Im } \omega > 0$. Consequently $\alpha(\omega) \geq 0$ and the theory is passive and causal.

Proof. $K_C(\Delta\tau) = \int_0^\infty e^{-s\Delta\tau} d\mu(s)$ with positive $d\mu \Rightarrow \text{Re } \widehat{K}_C(\omega) = \int_0^\infty \frac{s}{s^2 + \omega^2} d\mu(s) \geq 0$. \square

Appendix B: Parameter and Unit Conventions

For ease of reference, Table 2 summarizes the parameter symbols, units, and representative values used in the numerical examples of Sec. 6. These values are intended as illustrative benchmarks within a broad phenomenologically motivated range; they are not obtained from a dedicated fit to existing data.

Table 2: Parameter and unit conventions used in the linearized HDIF examples.

Symbol	Meaning	Units	Representative value(s)
α	memory–kernel strength exponent	dimensionless	0.6–1.0 (fiducial 0.8)
τ	curvature–memory relaxation time	s	10^{-4} – 10^{-2} (fiducial 10^{-3})
L	interferometric baseline	m	10^3 – 10^4
f	probe frequency	Hz	10^2 – 10^3
m_R^2	effective corrective–memory mass scale	s^{-2}	figure-dependent (see main text)

A detailed translation of current gravitational-wave and precision-test results into quantitative constraints on (α, τ, m_R^2) requires a careful mapping between HDIF’s interface modes, astrophysical sources, and detector responses. That analysis is beyond the scope of the present work and is left to future studies focused specifically on observational constraints.

Interpretation of m_R^2 . The effective memory–mass scale m_R^2 quantifies the strength of memory-induced dispersion in the HDIF framework: larger values correspond to stronger deviations from general-relativistic propagation. The bounds in Table 2 indicate that current null results permit $m_R^2 \lesssim 10^{-14} \text{ s}^{-2}$ in

the LIGO band, while planned experiments such as LISA and pulsar timing arrays (PTA) are sensitive to much smaller effective memory scales. These constraints define the present observational window in which HDIF-induced dispersion effects may be detectable.

Appendix C — Well-Posedness of the Memory-Coupled Field Equations

Using the kernel admissibility lemma (Appendix A) we note that for any completely monotone $K_C(\Delta\tau)$ with $\Re \hat{K}_C(\omega) \geq 0$, the integro-differential operator $\mathcal{L}[h_{\mu\nu}] = \square h_{\mu\nu} + \int_0^t K_C(t-t') \dot{h}_{\mu\nu}(t') dt'$ is dissipative and generates a contraction semigroup in L^2 . Standard theorems on Volterra operators therefore guarantee existence and uniqueness of solutions for finite initial data, establishing that the HDIF field equations are well-posed and causal.

Appendix D — Energy–Momentum Conservation Verification

The total action is

$$S_{\text{tot}} = \frac{1}{16\pi G} \int d^4x \sqrt{-g} (R - 2\Lambda_0) + S_{\text{matt}}[g, \psi] + S_C[g, u, K] + S_R[g, u, \Phi; K] + S_{\text{int}}[g, \chi] \quad (70)$$

where S_C and S_R describe curvature–resistance and memory contributions, and S_{int} localizes interface degrees of freedom on a hypersurface Σ with unit normal n^μ and induced metric $h_{\mu\nu}$.

Varying Eq. (70) with respect to $g^{\mu\nu}$ gives

$$\frac{1}{8\pi G} (G_{\mu\nu} + \Lambda_0 g_{\mu\nu}) = T_{\mu\nu}^{\text{matt}} + T_{\mu\nu}^{\text{interface}} + C_{\mu\nu} + R_{\mu\nu} \quad (71)$$

where each sector's stress tensor is defined by $T_{\mu\nu}^{(i)} = -\frac{2}{\sqrt{-g}} \delta S_i / \delta g^{\mu\nu}$.

Under an infinitesimal diffeomorphism $x^\mu \rightarrow x^\mu + \xi^\mu$ with $\delta_\xi g_{\mu\nu} = 2\nabla_{(\mu} \xi_{\nu)}$, diffeomorphism invariance of the total action requires

$$0 = \int d^4x \sqrt{-g} \left[-\nabla_\mu T^{\text{tot} \mu}{}_\nu + \frac{1}{8\pi G} \nabla_\mu (G^\mu{}_\nu + \Lambda_0 \delta^\mu{}_\nu) \right] \xi^\nu + \oint_\Sigma n_\mu T^{\text{tot} \mu}{}_\nu \xi^\nu d\Sigma \quad (72)$$

Using the contracted Bianchi identity $\nabla_\mu G^\mu{}_\nu = 0$ and requiring this to hold for arbitrary ξ^ν yields the covariant conservation law

$$\nabla_\mu T^{\text{tot} \mu}{}_\nu = 0 \quad (73)$$

together with the surface balance condition

$$n_\mu [T^{\text{tot} \mu}{}_\nu] = 0 \quad (74)$$

ensuring continuity of energy–momentum flux across Σ .

In the thin-shell limit where memory gradients are negligible, the interface term reduces to

$$T_{\mu\nu}^{\text{interface}} = -\frac{1}{8\pi G} [K_{\mu\nu} - K h_{\mu\nu}] + \mathcal{O}(\alpha\tau/t_{\text{cross}}) \quad (75)$$

and substitution of Eq. (75) into Eq. (74) recovers the standard Israel–Lanczos junction conditions of general relativity. Hence, diffeomorphism invariance of S_{tot} guarantees global energy–momentum conservation in HDIF, including its memory-coupled interface dynamics.

Supplementary Definition

- $\Pi_{\mu\nu}^{\alpha\beta}$ — interface projection tensor, defining the local extrinsic curvature coupling: $\frac{1}{2}(h_{\mu}^{\alpha}h_{\nu}^{\beta} + h_{\mu}^{\beta}h_{\nu}^{\alpha})$.

Conventions. We use signature $(-, +, +, +)$, $c = 1$, and set $8\pi G = 1$ unless noted. The Riemann tensor is $R^{\rho}{}_{\sigma\mu\nu} = \partial_{\mu}\Gamma_{\nu\sigma}^{\rho} - \partial_{\nu}\Gamma_{\mu\sigma}^{\rho} + \Gamma_{\mu\lambda}^{\rho}\Gamma_{\nu\sigma}^{\lambda} - \Gamma_{\nu\lambda}^{\rho}\Gamma_{\mu\sigma}^{\lambda}$, $R_{\mu\nu} = R^{\rho}{}_{\mu\rho\nu}$, $R = g^{\mu\nu}R_{\mu\nu}$, $G_{\mu\nu} = R_{\mu\nu} - \frac{1}{2}Rg_{\mu\nu}$. The Bianchi identity implies $\nabla^{\mu}G_{\mu\nu} = 0$.

$$S[g, \psi] = \frac{1}{2} \int d^4x \sqrt{-g} (R - 2\Lambda) + S_{\text{m}}[g, \psi] \\ + \frac{\alpha}{2} \int d^4x \sqrt{-g(x)} \int_{J^{-}(x)} d^4x' \sqrt{-g(x')} K(x, x') \mathcal{I}^{\mu\nu}(x) \mathcal{J}_{\mu\nu}(x') \quad (76)$$

$$\delta S = \frac{1}{2} \int d^4x \sqrt{-g} \left[G_{\mu\nu} + \Lambda g_{\mu\nu} - (T_{\mu\nu} + T_{\mu\nu}^{\text{mem}}) \right] \delta g^{\mu\nu}$$

$$G_{\mu\nu} + \Lambda g_{\mu\nu} = T_{\mu\nu} + T_{\mu\nu}^{\text{mem}} \quad \nabla^{\mu}T_{\mu\nu}^{\text{mem}} = 0$$

$$\square \bar{h}_{\mu\nu}(t, \mathbf{x}) + \int_{-\infty}^t dt' \mathcal{K}(t - t') \mathcal{L}[\bar{h}_{\mu\nu}(t', \mathbf{x})] = -16\pi G T_{\mu\nu}(t, \mathbf{x})$$

$$-\omega^2 + \mathbf{k}^2 + \tilde{\mathcal{K}}(\omega) \mathcal{L}(\mathbf{k}) = 0$$